The Role of Dynamic Ligand Exchange in the Oxidation Chemistry of Cerium(III)

Jerome R. Robinson,[a] Yusen Qiao,[a] Jun Gu,[a] Patrick J. Carroll,[a] Patrick J. Walsh,*[a] and Eric J. Schelter*[a]

[a] P. Roy and Diana T. Vagelos Laboratories, Department of Chemistry, University of Pennsylvania, Philadelphia, PA 19104, United States
Phone: (+1)-(215)-898-8633, (+1)-(215)-573-2875; e-mail: schelter@sas.upenn.edu, pwalsh@sas.upenn.edu

Supporting Information

Experimental Procedures

General Methods. For all reactions and manipulations performed under an inert atmosphere (N_2), standard Schlenk techniques or a Vacuum Atmospheres, Inc. Nexus II drybox equipped with a molecular sieves 13X / Q5 Cu–0226S catalyst purifier system were used. Glassware was oven-dried overnight at 150 °C prior to use. ^{1}H-NMR spectra were obtained on a Brüker AM-500, Brüker UNI-400, or a Brüker DMX-300 Fourier transform NMR spectrometer at 500, 400, or 300 MHz, respectively. ^{13}C{^{1}H}-NMR spectra were recorded on a Brüker AM-500 or a Brüker DMX-300 Fourier transform NMR spectrometer at 126 or 76 MHz respectively. ^{7}Li-NMR spectra were recorded on a Brüker AM-500 or Brüker UNI-400 Fourier transform NMR spectrometer at 194 or 155 MHz respectively. All spectra were measured at 300 K unless otherwise specified. Chemical shifts were recorded in units of parts per million downfield from residual proteo solvent peaks (^{1}H-) or characteristic solvent peaks (^{13}C{^{1}H}). The ^{7}Li spectra were referenced to external solution standards of LiCl in H_2O (at zero ppm). All coupling constants are reported in hertz. The infrared spectra were obtained from 400-4000 cm^{-1} using a Perkin Elmer 1600 series infrared spectrometer. Elemental analyses were performed at the University of California, Berkeley Microanalytical Facility using a Perkin-Elmer Series II 2400 CHNS analyzer.

Materials. Tetrahydrofuran, diethyl ether, dichloromethane, hexanes, and pentane were purchased from Fisher Scientific. The solvents were sparged for 20 min with dry N_2 and dried using a commercial two-column solvent purification system comprising columns packed with Q5 reactant and neutral alumina respectively (for hexanes and pentane), or two columns of neutral alumina (for THF, Et_2O and CH_2Cl_2). Deuterated tetrahydrofuran and pyridine were purchased from Cambridge Isotope Laboratories, Inc. Deuterated tetrahydrofuran was stored for at least 12 h over potassium mirror, whereas pyridine was stored over 4 Å molecular sieves prior to use. Li[N($SiMe_3$)$_2$] was purchased from Sigma Aldrich and was recrystallized from hot pentane prior to use. (*S*)-BINOL and $CeCl_3$ (>99.9% purity) were purchased from AKScientific and Strem, respectively, and used without additional purification. Trityl chloride was purchased from Acros Organics and used without further purification. Ce[N($SiMe_3$)$_2$]$_3$,[1]

$[Li_3(THF)_6][(BINOLate)_3Yb]$ (**1–Yb(het)** and **1–Yb(homo)**),[2] and **1–Ce(homo)**,[2c, 3] **2–Ce–Cl(homo)**,[2c, 3] and $[^nPr_4N][B(3,5\text{-}(CF_3)_2\text{-}C_6H_3)_4]$,[4] were prepared according to literature procedures.

2D Exchange Spectroscopy (EXSY) NMR Experiments

All 2D ^1H and ^7Li-NMR EXSY experiments were performed on a Brüker UNI-400 Fourier transform NMR spectrometer at 400 and 155 MHz respectively using THF–d_8 as a solvent (sample concentrations listed below) and a conventional NOESY sequence. 2048 and 1024 data points were used in the t_2 and t_1 domain respectively, where 8 scans were collected for each slice with the exception of the ^7Li-NMR EXSY experiment for **1–Ce(het)** (32 scans). Several t_{mix} were used for EXSY experiments performed at 300 K to determine the optimal value for each relevant exchange pathway. In addition to the values of t_{mix} listed, a reference was recorded at t_{mix} = 0 ms. Pseudo-first order rate constants (k, s^{-1}) were calculated using EXSYCalc 1.0 (Mestrelab Research)[5] from volume intensities obtained from the 2D spectra. Activation parameters were determined using Eyring plots generated from rate data obtained at several temperatures.

UV-Vis Absorption Spectroscopy and Kinetics. All UV-Vis Absorption measurements and pseudo-first order kinetics studies were performed using a Perkin Elmer 950 UV-Vis/NIR spectrophotometer. 1 mm pathlength screw cap quartz cells were used with a blank measured before each run. All samples were prepared under an N_2 atmosphere (see General Experimental above). Pseudo-first order kinetics studies for **1–Ce** were observed to 3 $t_{1/2}$ at 487 nm. All pseudo-first order kinetics measurements gave fits (R^2) ≥ 0.999 following a first order integrated rate law.

Note: Our proposed mechanism implies the formation of **2–Ce-Cl(homo)** as an intermediate to the formation of **2–Ce(het)**. Although ε values for these two compounds are fairly similar at 487 nm (~5% difference; **2–Ce(het)** ε = 8691 $M^{-1}\cdot cm^{-1}$; **2–Ce-Cl(homo)**: ε = 8270 $M^{-1}\cdot cm^{-1}$), if **2–Ce-Cl(homo)** were to build up during the rate studies an underestimation of k_{obs} would occur. In the worst case scenario, which assumes that all of the Ce^{IV} species in solution corresponded to **2–Ce-Cl(homo)** instead of **2–Ce(het)**, a 12% error in k_{obs} would be observed.

Electrochemistry. Voltammetry experiments were performed using a CH Instruments 620D Electrochemical Analyzer/Workstation and the data were processed using CHI software v 9.24. All experiments were performed in an N_2 atmosphere drybox using electrochemical cells that consisted of a 4 mL vial, glassy carbon (3 mm diameter) working electrode, a platinum wire counter electrode, and a silver wire plated with AgCl as a quasi-reference electrode. The working electrode surfaces were polished prior to each set of experiments, and were periodically replaced on scanning > 0 V versus ferrocene (Fc) to prevent the buildup of oxidized product on the electrode surfaces. Solutions employed during CV studies were ~1 mM in analyte and 100 mM in [^{n}Pr$_4$N][B(3,5-(CF$_3$)$_2$-C$_6$H$_3$)$_4$] ([^{n}Pr$_4$N][BAr$^F{}_4$]). Potentials were reported versus Fc, which was added as an internal standard for calibration at the end of each run. All data were collected in a positive-feedback IR compensation mode. The cell resistances measured with THF as a solvent were ≤ 500 Ω. Scan rate dependences of 25–1000 mV/s were performed to determine electrochemical reversibility.

X-Ray Crystallography. X-ray intensity data were collected on a Brüker APEXII CCD area detector employing graphite-monochromated Mo-Kα radiation (λ=0.71073 Å) at a temperature of 143(1)K. In all cases, rotation frames were integrated using SAINT,[6] producing a listing of unaveraged F^2 and $\sigma(F^2)$ values which were then passed to the SHELXTL[6] program package for further processing and structure solution on a Dell Pentium 4 computer. The intensity data were corrected for Lorentz and polarization effects and for absorption using TWINABS[7] or SADABS.[8] The structures were solved by direct methods (SHELXS-97).[9] Refinement was by full-matrix least squares based on F^2 using SHELXL-97.[9] All reflections were used during refinements. Non-hydrogen atoms were refined anisotropically and hydrogen atoms were refined using a riding model. Crystallographic data and structure refinement information are summarized in **Table S3.** The crystallographically determined bond lengths and angles for **1–Ce(het)** and **2–Ce(het)** are displayed in **Tables S5** and **S6**.

Synthetic Details and Characterization

Synthesis of 1–Ce(het) A 20 mL scintillation vial was charged with Ce[N(SiMe$_3$)$_2$]$_3$ (455.1 mg, 0.732 mmol; FW: 621.27), THF (6 mL), and a Teflon-coated stir bar. (*rac*)–BINOL (629.9 mg, 2.20 mmol, 3

equiv, FW: 286.32) was added as a solid to the clear light-yellow solution, which resulted in a light yellow precipitate/slurry. $LiN(SiMe_3)_2$ (367.4 mg, 2.20 mmol, 3 equiv; FW: 167.32) was added as a solid, resulting in an immediate color change to orange and dissolution of precipitate. The reaction was stirred for an additional two hours and then filtered through a Celite-packed coarse porosity fritted filter. Bright yellow-orange crystals were grown from layering concentrated THF solutions of **1–Ce(het)** with hexanes (1:5 v/v) and allowing the vial(s) to sit undisturbed for 12 – 36 h at –30 °C. The crystals were isolated by vacuum filtration over a medium porosity fritted filter and dried for 3 h under reduced pressure. 781.4 mg (0.540 mmol, 74% yield; FW: 1446.52). Anal. Calcd for $C_{84}H_{84}O_{12}Li_3Ce$: C, 69.75; H, 5.85. Found: C, 69.69; H, 5.66. Bright yellow X-ray quality single crystals were obtained by layering concentrated solutions of **1–Ce(het)** with hexanes (1:5 v/v) at –30 °C. ^{1}H-NMR (500 MHz, THF–d_8) δ 15.17 (s, 2H; het), 10.14 (s, 2H; het), 9.98 (d, J = 8.2 Hz, 6H; homo), 8.77 (s, 2H; het), 8.62 (t, J = 10.5 Hz, 9H; het), 8.07 (t, J = 7.7 Hz, 6H; homo) 7.52 (d, J = 7.8 Hz, 6H; homo), 7.45 (t, J = 7.5 Hz, 6H; homo), 7.11 (s, 2H; het), 6.82 (s, 2H; het), 5.59 (s, 6H; homo), 5.50 (s, 2H; het), 5.32 (s, 2H; het), 4.19 (s, 4H; het), 2.23 (s, 4H; het), –1.87 (s, 6H; homo), –3.38 (s, 2H; het), –7.83 (s, 2H; het), –11.58 (s, 2H; het). ^{7}Li-NMR (155 MHz, THF–d_8) δ 62.9 (1Li; het), 19.6 (3Li; homo), 11.3 (2Li; het). ^{13}C{^{1}H}-NMR (126 MHz, THF–d_8) δ 193.3 (het), 171.0 (homo), 151.4 (het), 148.0 (het), 140.0 (homo), 135.3 (het), 134.7 (het), 130.7 (homo), 130.3 (homo), 130.1 (homo), 128.5 (2C het + homo), 126.1 (homo), 125.8 (homo), 125.2 (het), 124.9 (homo), 123.6 (het), 121.7 (homo). **Note**: Nine of the possible 30 ^{13}C resonances were observed for **1–Ce(het)**, which we attribute to peak overlap (accidental equivalence) and line broadening (ligand exchange processes and the paramagnetic Ce^{III}) cation. ^{1}H-NMR (400 MHz, Pyr–d_5) 10.09 (d, J = 8.3 Hz, 6H; homo), 8.06 (t, J = 7.5 Hz, 6H; homo), 7.80 (d, J = 7.8 Hz, 6H; homo), 7.58 (m, 6H; homo), 6.50 (d, J = 6.4 Hz, 6H; homo), 3.86 (s, 6H; homo). ^{7}Li-NMR (155 MHz, THF–d_8) δ 23.1. IR (Nujol, cm^{-1}) ν: 2953, 2924, 2855, 1613, 1588, 1554, 1498, 1462, 1422, 1376, 1366, 1340, 1273, 1246, 1238, 1209, 1179, 1139, 1125, 1071, 1045, 993, 959, 937, 891, 860, 823, 774, 743, 691, 666, 632, 592, 575, 533, 522, 498, 477, 421.

Synthesis of (*RRR*)**-2–Ce-Cl(homo).** A 20 mL vial was charged with (*RRR*)**-1–Ce(homo) (**200.0 mg, 0.138 mmol; FW: 1446.5 g·mol^{-1}), THF (3 mL), and a Teflon-coated stir bar. Trityl chloride (38.5 mg, 0.138 mmol, 1 equiv; FW: 278.78 g·mol^{-1}) was added as a solid to the clear stirring solution. Upon addition, an immediate color change from pale yellow to dark purple was observed, and the reaction was stirred for 2 h at room temperature. The reaction was filtered through a Celite-packed pipette and THF solvent was removed from the filtrate under reduced pressure to yield a purple residue. Dissolving the residue in minimal THF (2 mL) followed by layering with pentane (1:4 v/v) yielded dark purple crystals after 24 h. The crystals were isolated by vacuum filtration over a medium porosity fritted filter, washed with pentane (3 x 5 mL), and dried for 3 h under reduced pressure. Yield: 178 mg (0.120 mmol, 87%, FW: 1481.95 g·mol^{-1}). Spectroscopic characterization matched that of (*SSS*)**-2–Ce-Cl(homo)**.[2c] ^{1}H-NMR(400 MHz, THF–d_8) δ: 7.63 (d, *J* = 6.5 Hz, 6H), 7.39 (s, br, 6H), 7.00 (s, 6H), 6.92 (s, 6H), 6.88 (s, 6H), 6.87 (s, br, 6H). ^{7}Li-NMR (155 MHz, THF–d_8) δ: –1.68.

Synthesis of 2–Ce(het)·0.5C$_5$H$_{12}$. A 20 mL scintillation vial was charged with **1–Ce(het)** (250.0 mg, 0.173 mmol, FW: 1446.52 g·mol^{-1}), THF (5 mL), and a Teflon-coated stir bar. Trityl chloride (48.2 mg, 0.173 mmol, 1 equiv; FW: 278.78 g·mol^{-1}) was added as a solid to the stirred THF solution. Upon addition of trityl chloride, the solution instantly changed from pale yellow to dark purple. The reaction was stirred at room temperature for 1 h, filtered through a Celite-packed coarse porosity fritted filter, and the solvent was removed from the filtrate under reduced pressure to yield a purple residue. The purple residue was then extracted with toluene (8 mL). The dark purple solution was filtered through a Celite-packed coarse porosity fritted filter, and the solvent was removed from the filtrate under reduced pressure. Dark purple crystals were grown from layering concentrated THF solutions of **2–Ce(het)** with pentane (1:5 v/v) and allowing the vial(s) to sit undisturbed for 12 h at RT. The crystals were isolated by vacuum filtration over a medium porosity fritted filter and dried for 3 h under reduced pressure to yield 224.0 mg (0.168 mmol, 97% yield; FW: 1331.44 g·mol^{-1}). Anal. Calcd for $C_{78.5}H_{74}O_{10}Li_3Ce$: C, 70.47; H, 5.29. Found: C, 70.82; H, 5.60. ^{1}H-NMR (500 MHz, THF–d_8) δ 7.83 (d, *J* = 8.8 Hz, 2H), 7.74 (d, *J* = 8.1 Hz, 2H), 7.57 (d, *J* = 8.1 Hz, 1H), 7.50 (t, *J* = 8.3 Hz, 6H), 7.21 (d, *J* = 8.7 Hz, 1H), 7.05 – 6.75 (m, 23 H),

6.61 (d, J = 8.7 Hz, 1H). ^{7}Li-NMR (155 MHz, THF–d_8) δ 0.61. ^{13}C{^{1}H}-NMR (126 MHz, THF–d_8) δ 161.9, 161.5, 135.7, 135.4, 130.4, 130.2, 130.1, 128.8, 128.5, 128.2, 128.2, 128.0, 127.6, 127.5, 127.5, 125.4, 125.3, 125.1, 125.0, 124.7, 122.3, 122.3, 119.7, 119.0. **Note**: 22 of the possible 30 ^{13}C resonances were observed for **2–Ce(het)**, which we attribute to peak overlap (accidental equivalence). IR (KBr, cm^{-1}) *v*: 3052, 3033, 2976, 2954, 885, 2873, 1615, 1589, 1559, 1501, 1460 , 1424, 1365, 1352, 1333, 1271, 1240, 1145, 1071, 1046, 992, 954, 912, 893, 858, 818, 744, 689, 665, 590, 573, 541, 499, 479. Dark purple X-ray quality single crystals were grown from layering concentrated THF solutions of **2–Ce(het)** with pentane (1:5 v/v).

References

1. Bradley, D. C.; Ghotra, J. S.; Hart, F. A., *J Chem Soc Dalton* **1973**, 1021-1027.
2. (a) Di Bari, L.; Lelli, M.; Pintacuda, G.; Pescitelli, G.; Marchetti, F.; Salvadori, P., *J. Am. Chem. Soc.* **2003,** *125*, 5549-5558. (b) Wooten, A. J.; Carroll, P. J.; Walsh, P. J., *J. Am. Chem. Soc.* **2008,** *130*, 7407-7419. (c) Robinson, J. R.; Carroll, P. J.; Walsh, P. J.; Schelter, E. J., *Angew Chem Int Edit* **2012,** *51*, 10159-10163. (d) Robinson, J. R.; Gordon, Z.; Booth, C. H.; Carroll, P. J.; Walsh, P. J.; Schelter, E. J., *J. Am. Chem. Soc.* **2013,** *135*, 19016-19024.
3. Robinson, J. R.; Gordon, Z.; Booth, C. H.; Carroll, P. J.; Walsh, P. J.; Schelter, E. J., *J. Am. Chem. Soc.* **2013,** *135*, 19016-19024.
4. Thomson, R. K.; Scott, B. L.; Morris, D. E.; Kiplinger, J. L., *Comptes Rendus Chimie* **2010,** *13*, 790-802.
5. Cobas, J. C.; Martin-Pastor, M. *EXSYCalc*, 1.0; Mestrelab Research: Santiago De Compostela.
6. Bruker, SHELXTL. Bruker AXS Inc.: Madison, Wisconsin, USA, 2009.
7. Sheldrick, G. M., TWINABS. University of Gottingen, Germany, 2008.
8. Sheldrick, G. M., SADABS. University of Gottingen, Germany, 2007.
9. Sheldrick, G. M., *Acta Crystallogr A* **2008,** *64*, 112-122.

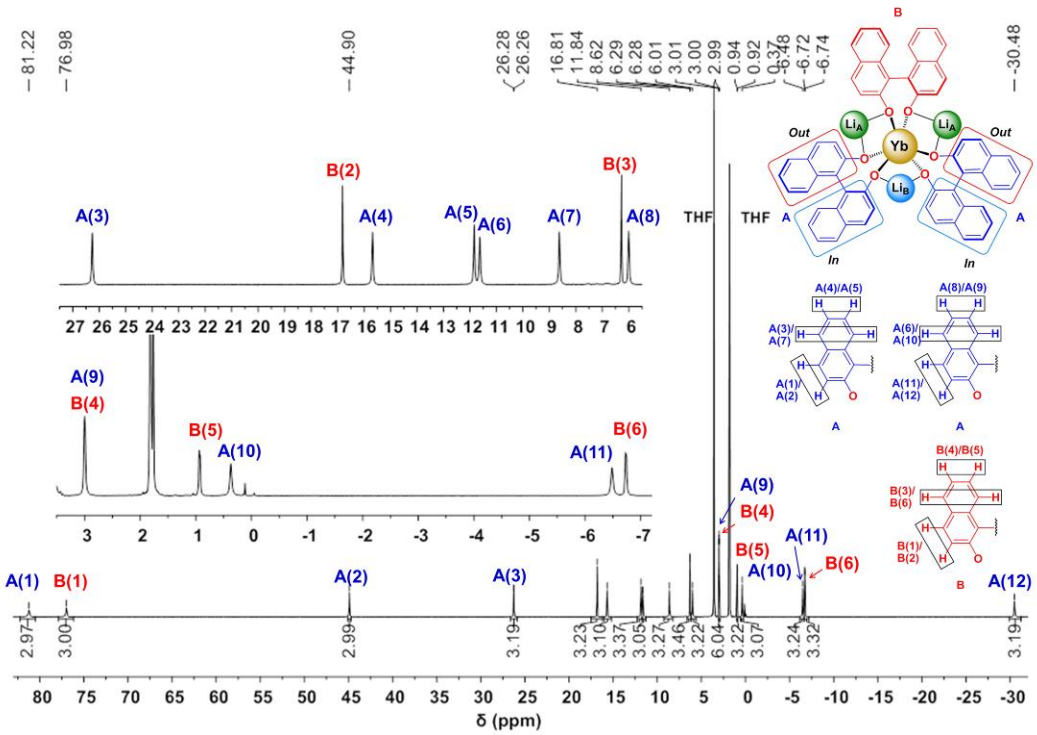

Figure S1a. ^{1}H-NMR(400 MHz, THF–d_8) of **1–Yb(het)**.

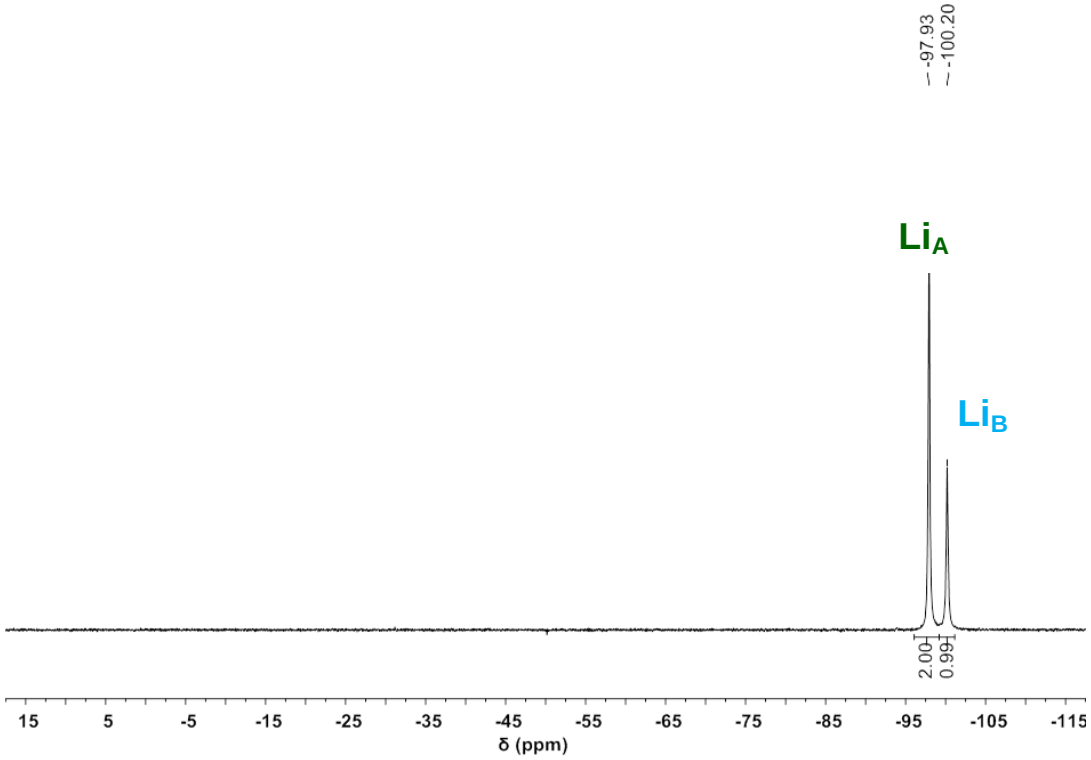

Figure S1b. ^{7}Li-NMR(155 MHz, THF–d_8) of **1–Yb(het)**.

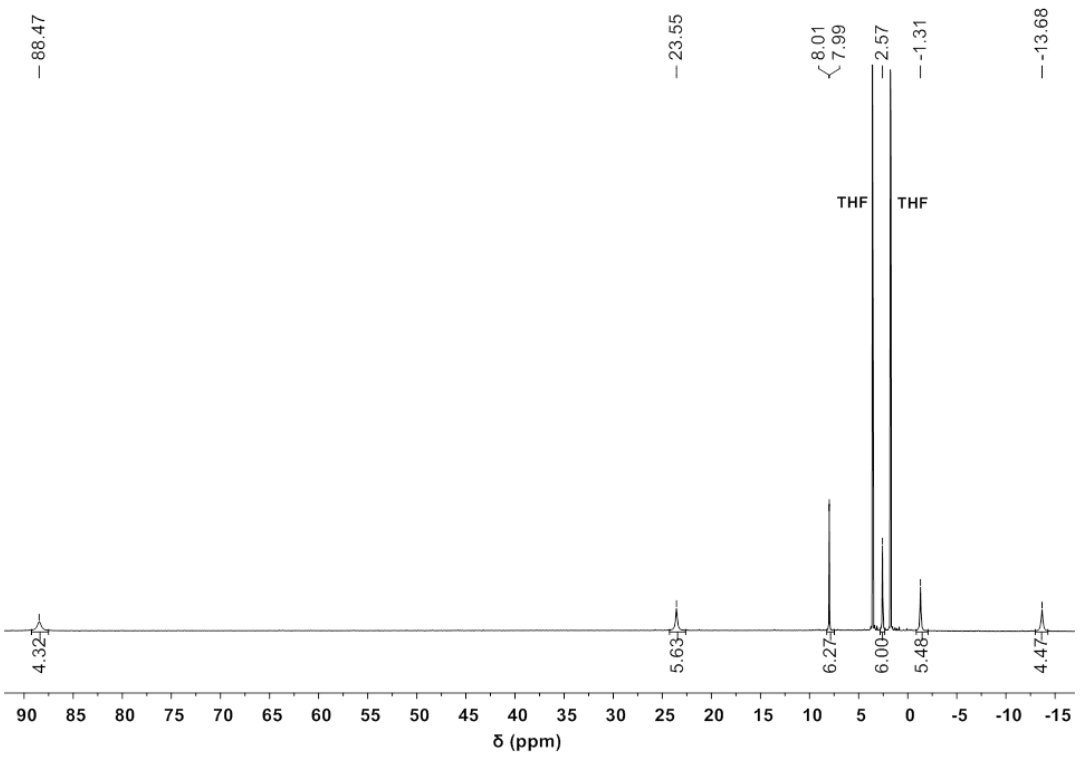

Figure S2a. ^{1}H-NMR(400 MHz, THF–d_8) of **1–Yb(homo)**.

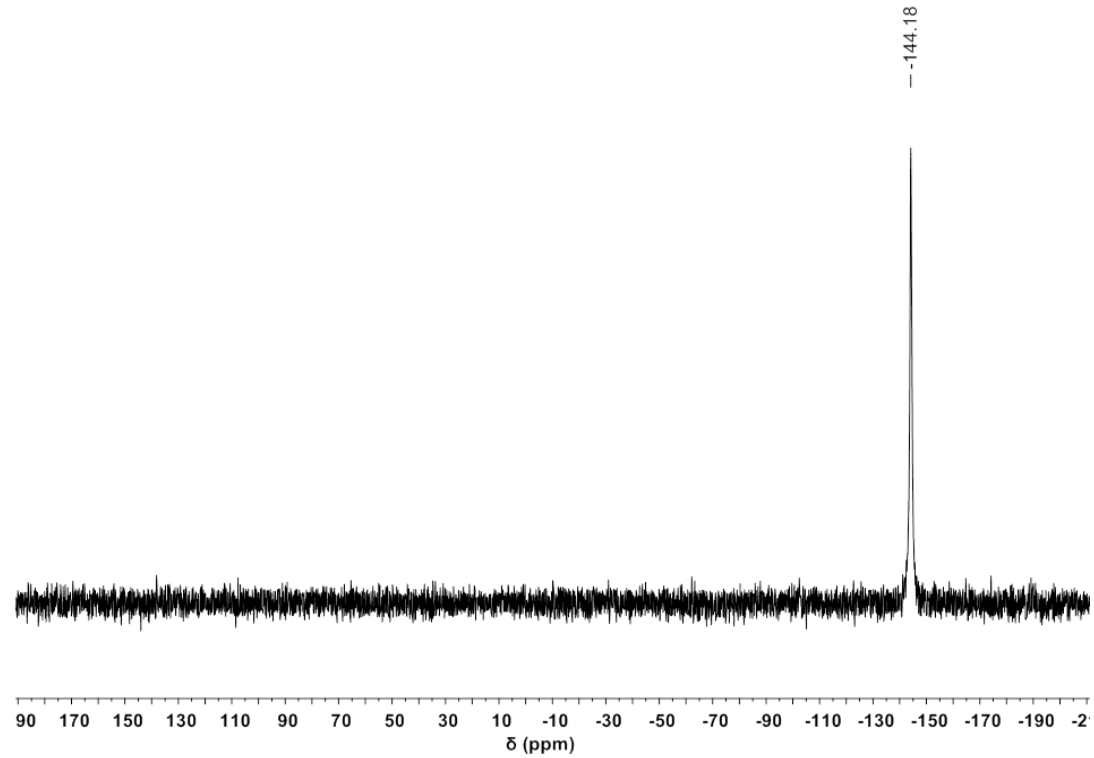

Figure S2b. ^{7}Li{^{1}H}-NMR(155 MHz, THF–d_8) of **1–Yb(homo)**.

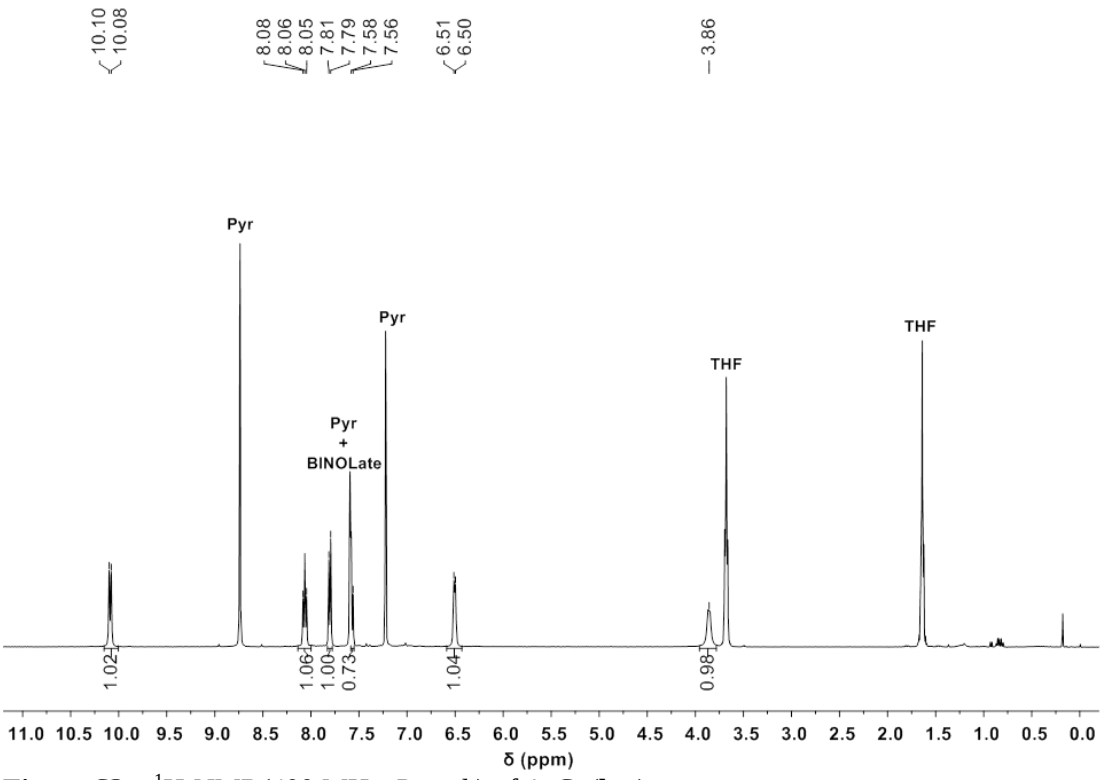

Figure S3a. ^{1}H-NMR(400 MHz, Pyr–d_5) of **1–Ce(het)**.

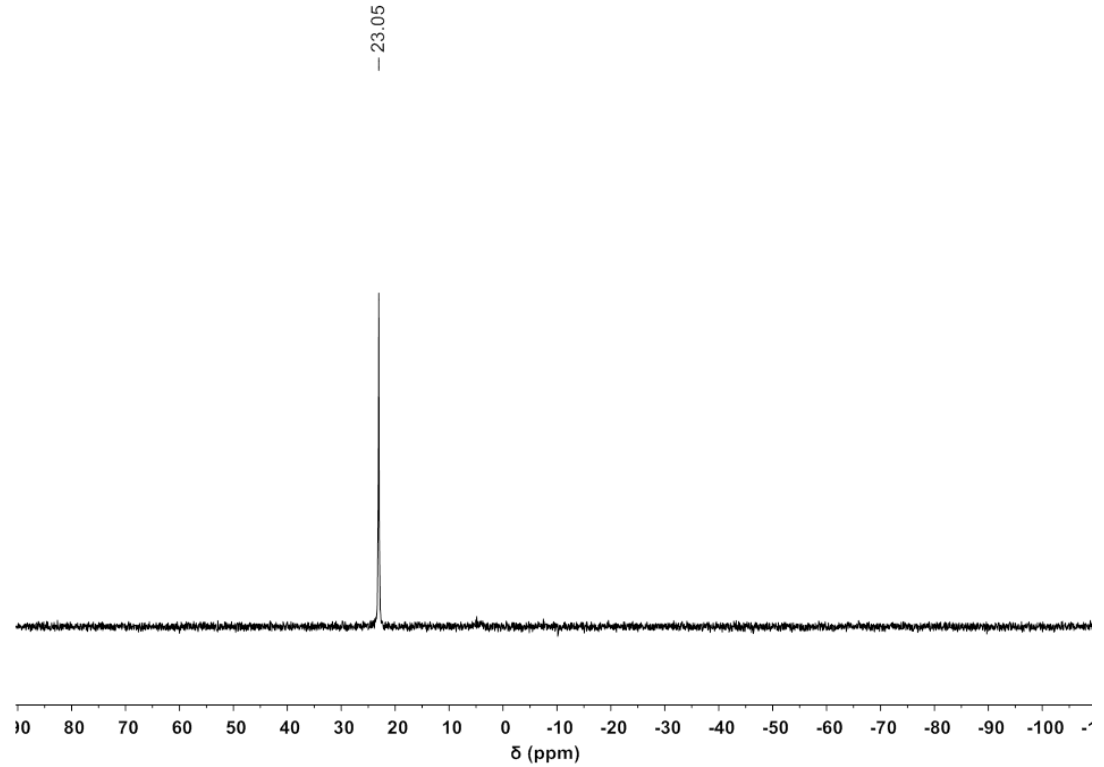

Figure S3b. ^{7}Li-NMR(155 MHz, Pyr–d_5) of **1–Ce(het)**.

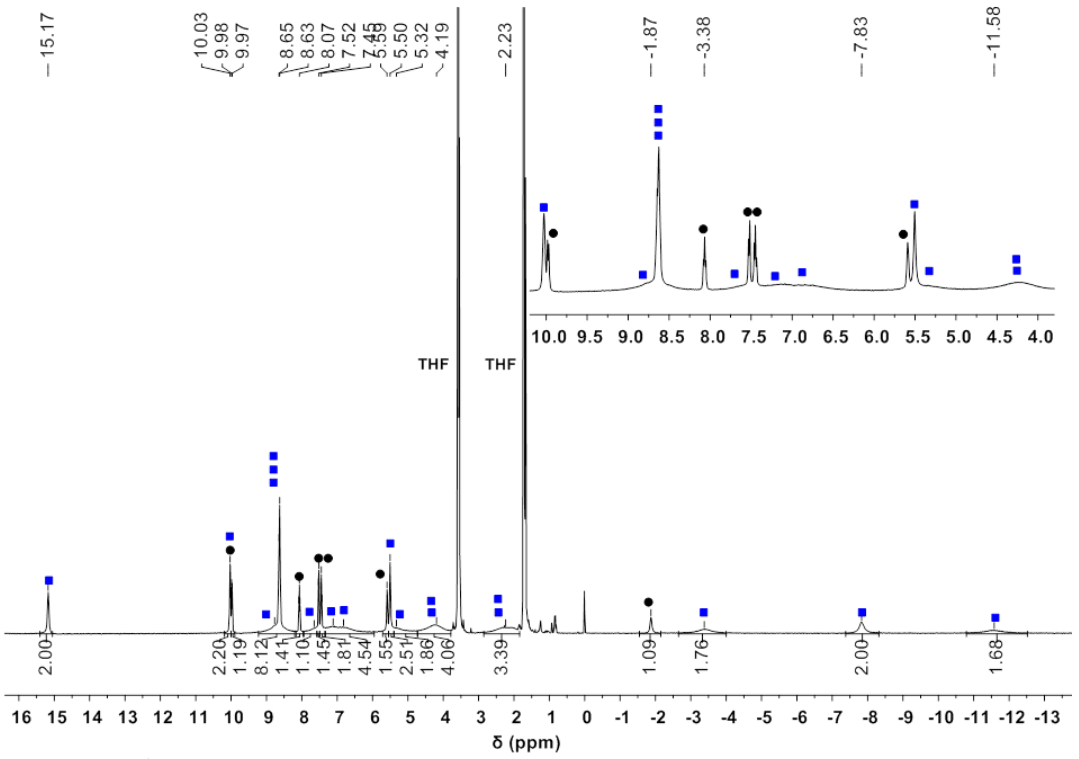

Figure S4a. ^{1}H-NMR(500 MHz, THF–d_8) of **1–Ce(het)**. ■ = **1–Ce(het)**, ♦ = **1–Ce(homo)**.

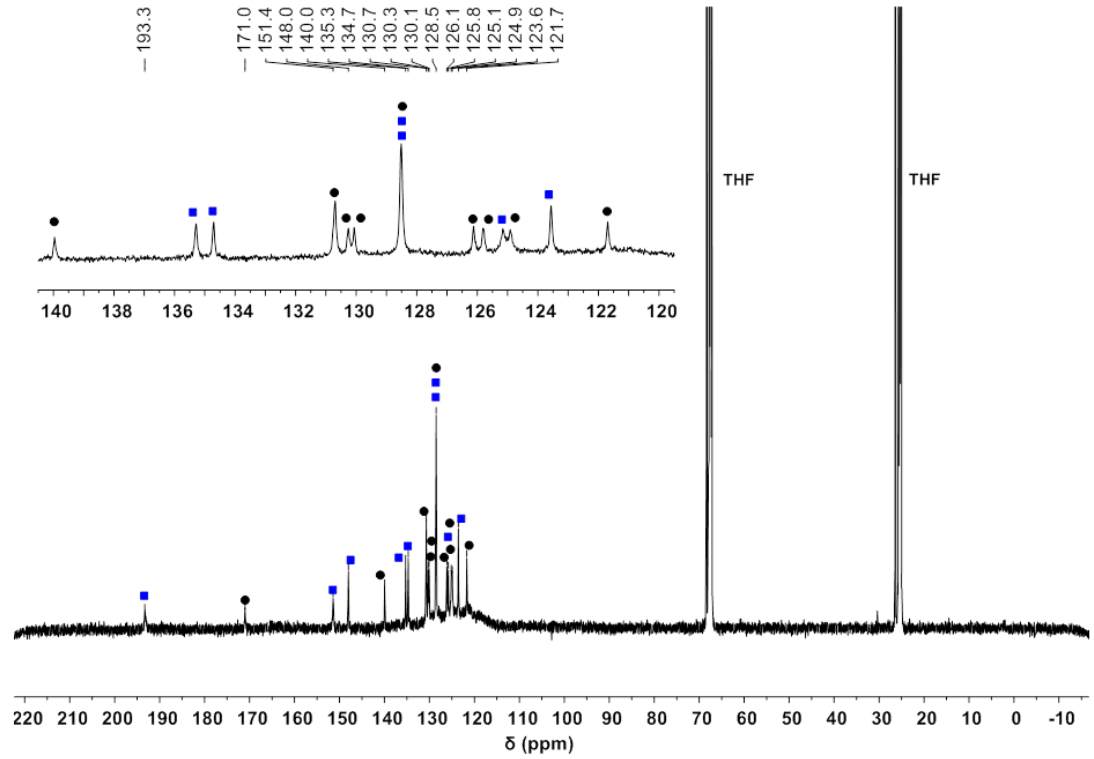

Figure S4b. ^{13}C{^{1}H}-NMR(126 MHz, THF–d_8) of **1–Ce(het)**. ■ = **1–Ce(het)**, ♦ = **1–Ce(homo)**.

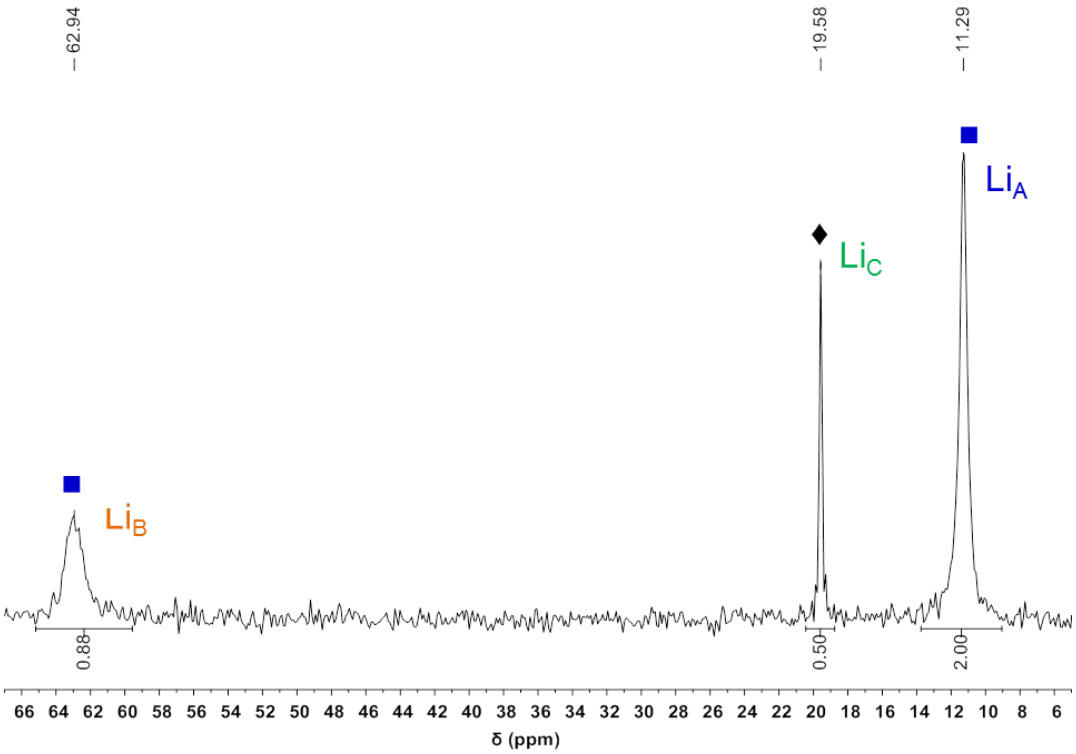

Figure S4c. ^{7}Li-NMR(155 MHz, THF–d_8) of **1–Ce(het)**. ■ = **1–Ce(het)**, ♦ = **1–Ce(homo)**.

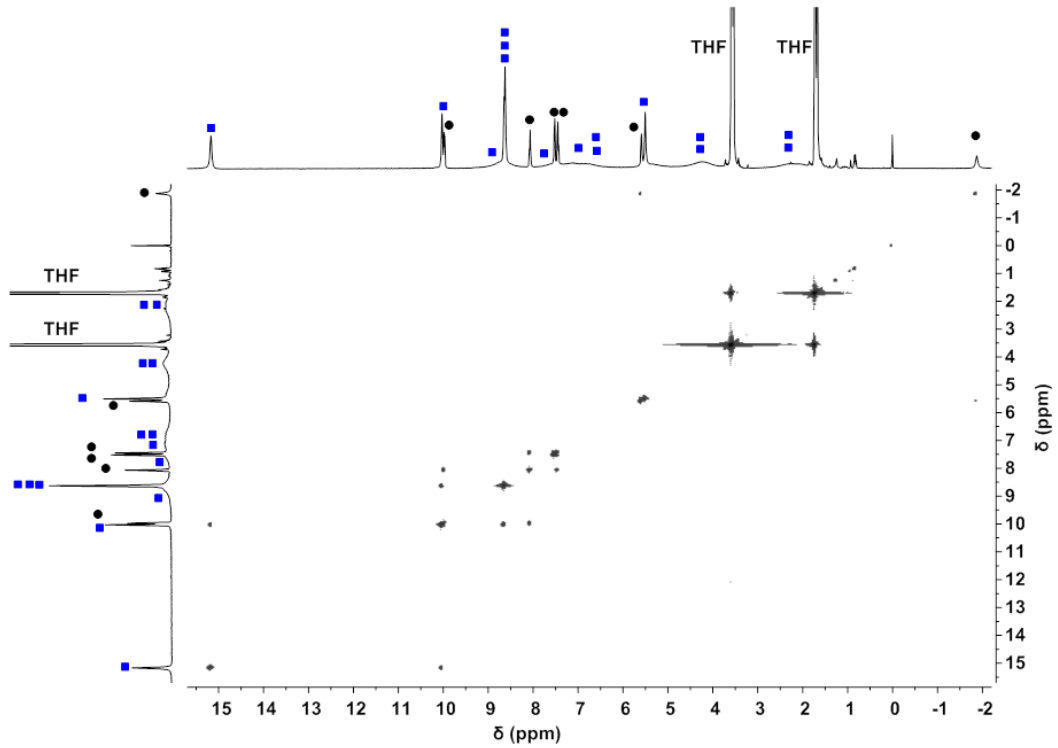

Figure S5. ^{1}H COSY-NMR spectrum (500 MHz, THF–d_8) of **1–Ce(het)** (**1–Ce** = 0% ee). ■ = **1–Ce(het)**, ♦ = **1–Ce(homo)**.

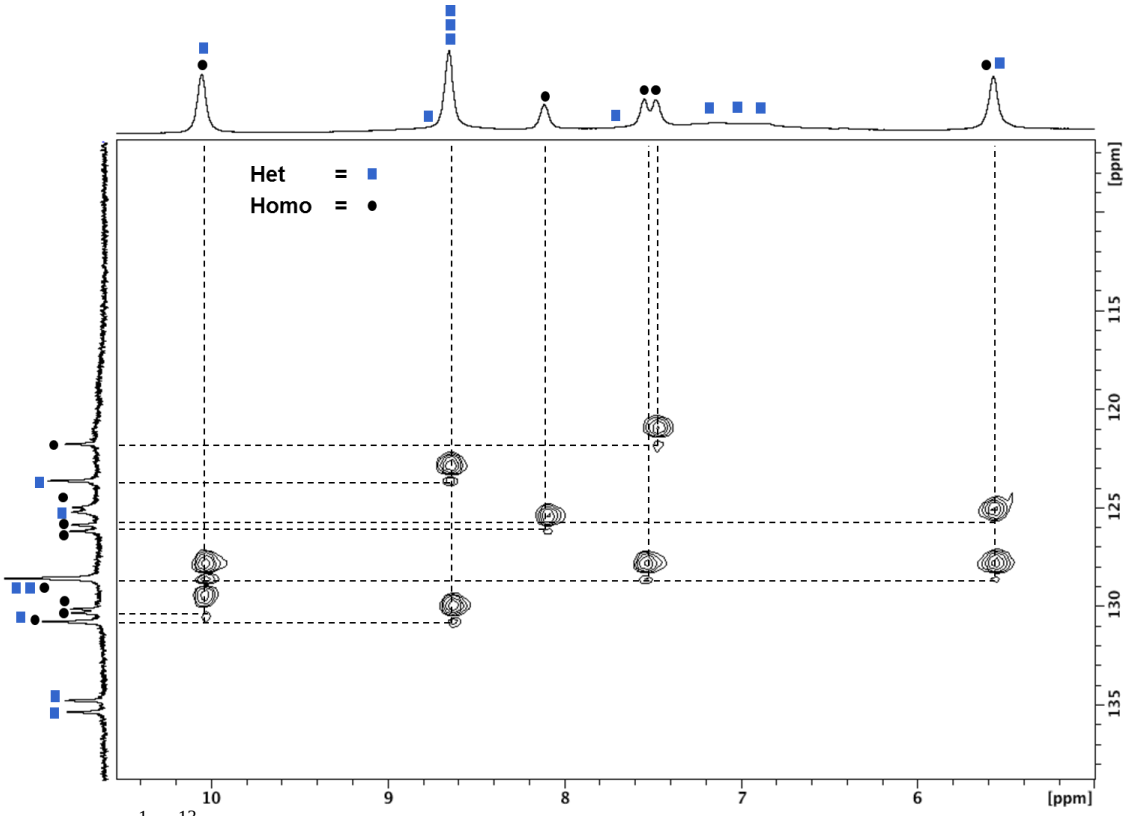

Figure S6. ^{1}H-^{13}C HSQC-NMR spectrum (500 MHz, THF–d_8) of **1–Ce(het)** (**1–Ce** = 0% ee). Dashed lines provided a guide for the eye to identify cross peaks. ■ = **1–Ce(het)**, ♦ = **1–Ce(homo)**.

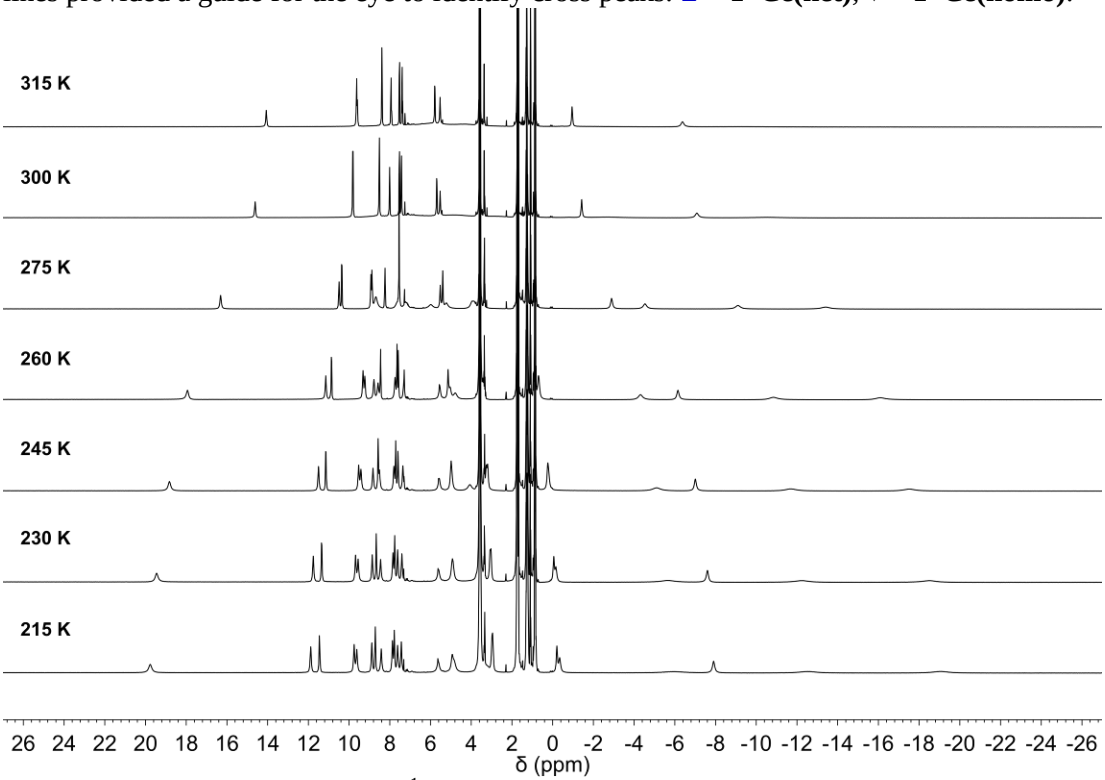

Figure S7a. Variable temperature ^{1}H-NMR (400 MHz, THF–d_8) of **1–Ce(het)** (**1–Ce** = 0% ee).

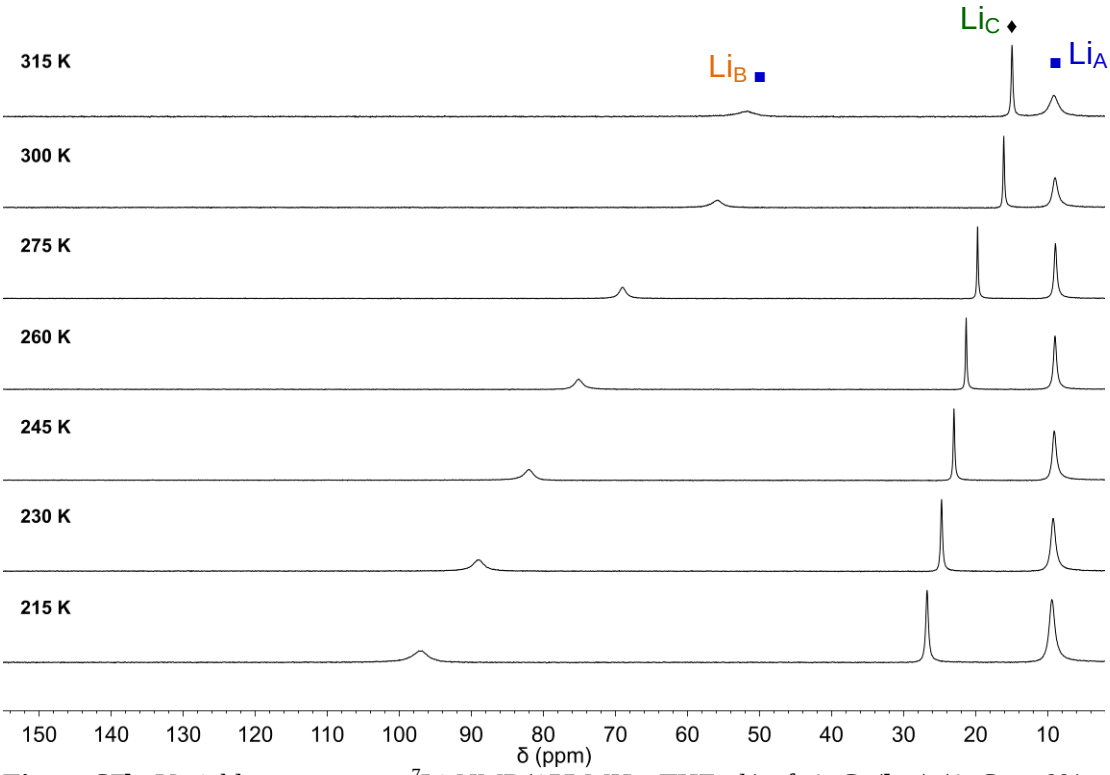

Figure S7b. Variable temperature ^{7}Li-NMR(155 MHz, THF–d_8) of **1–Ce(het)** (**1–Ce** = 0% ee). ■ = **1–Ce(het)**, ♦ = **1–Ce(homo)**.

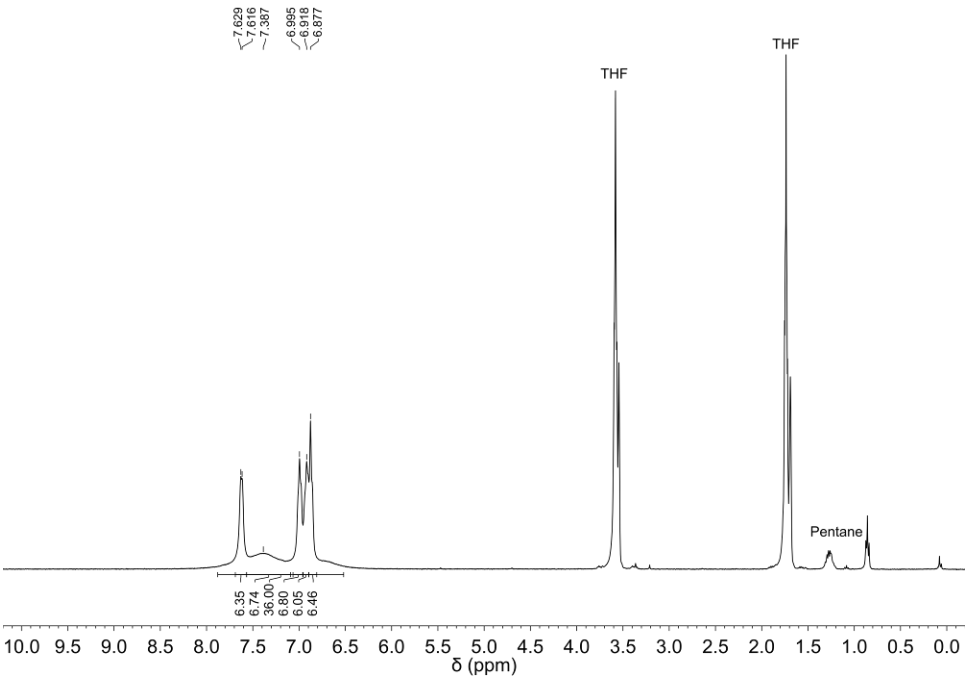

Figure S8a. ^{1}H-NMR (400 MHz, THF–d_8) of (*RRR*)-**2–Ce-Cl(homo)**.

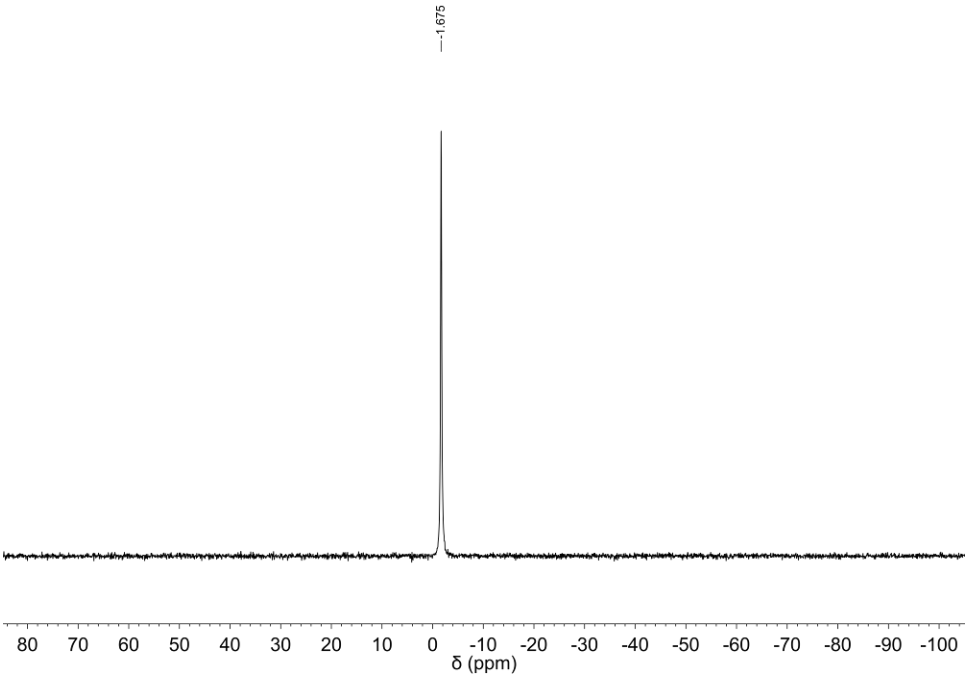

Figure S8b. ^{7}Li-NMR(155 MHz, THF–d_8) of (*RRR*)-**2–Ce-Cl(homo)**.

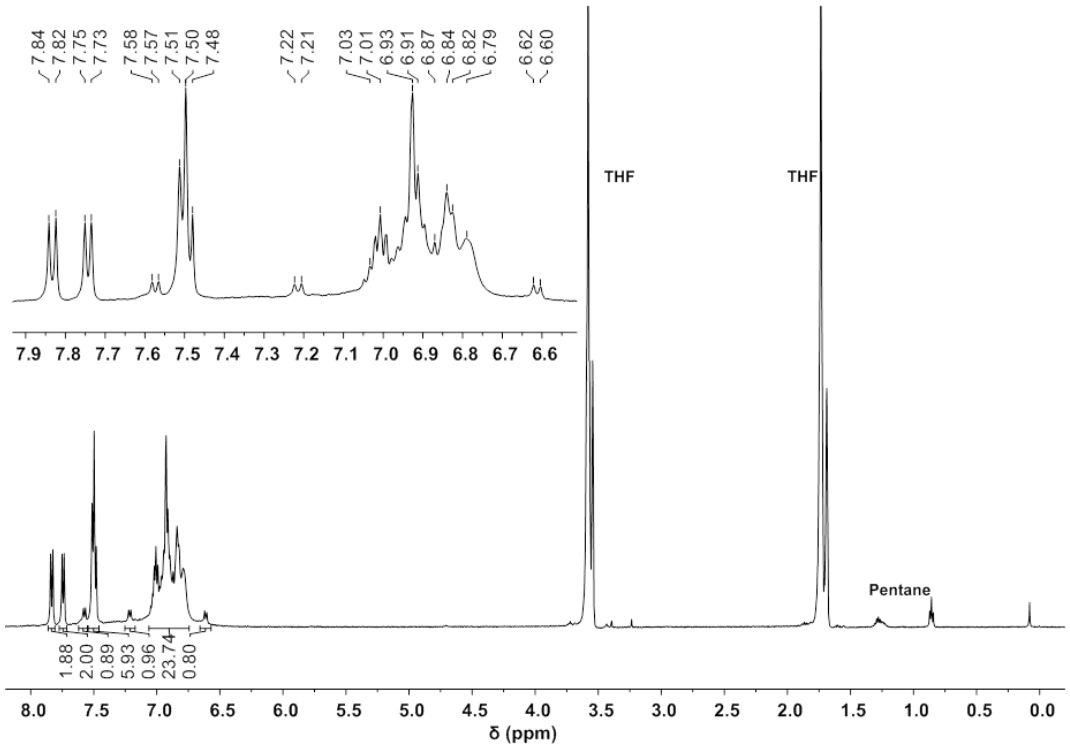

Figure S9a. ^{1}H-NMR(500 MHz, THF–d_8) of **2–Ce(het)**.

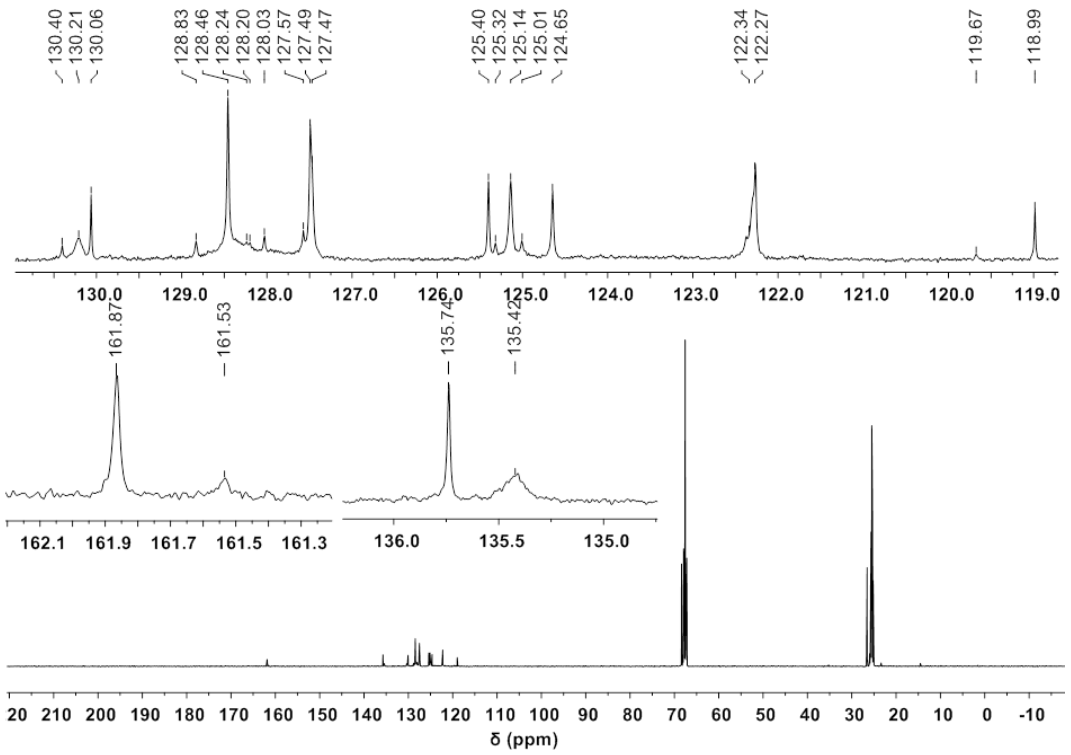

Figure S9b. $^{13}C\{^{1}H\}$-NMR(126 MHz, THF–d_8) of **2–Ce(het)**.

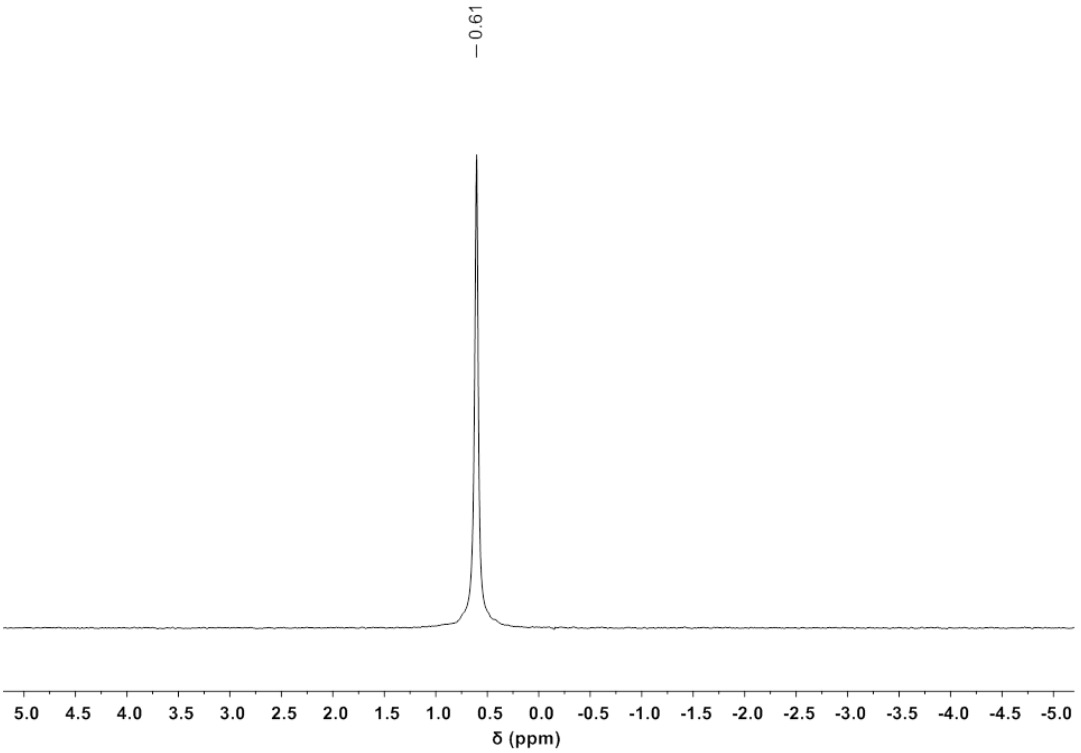

Figure S9c. ^{7}Li-NMR(155 MHz, THF–d_8) of **2–Ce(het)**.

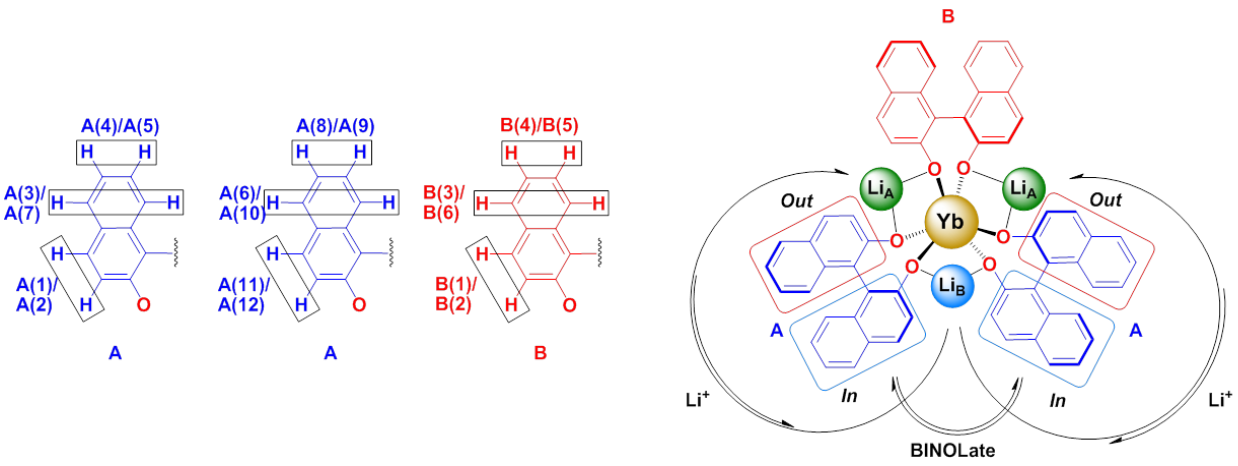

Figure S10. Spin systems and exchange processes identified in **1–Yb(het)** by 1H COSY- and EXSY-NMR.

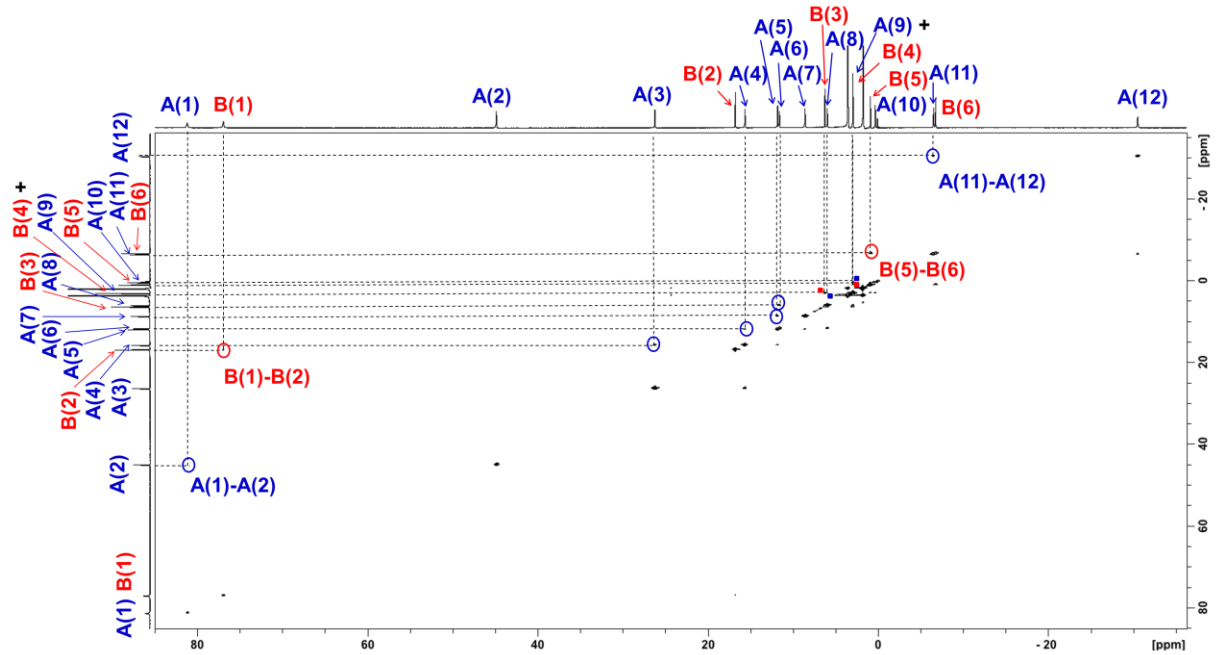

Figure S11a. ^{1}H COSY-NMR of **1–Yb(het)** (19.3 mM; t_{mix} = 5 ms, 300 K; **1–Yb** = 0% ee) taken in THF–d_8.

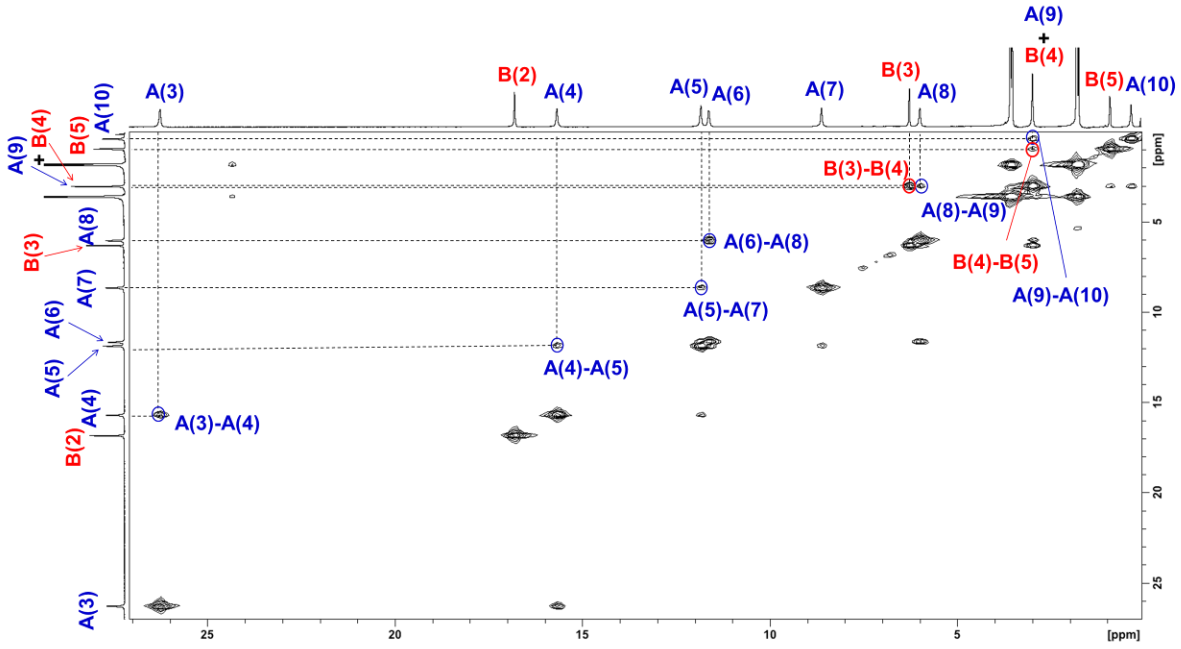

Figure S11b. ^{1}H COSY-NMR of **1–Yb(het)** (19.3 mM; t_{mix} = 5 ms, 300 K; **1–Yb** = 0% ee) taken in THF–d_8.

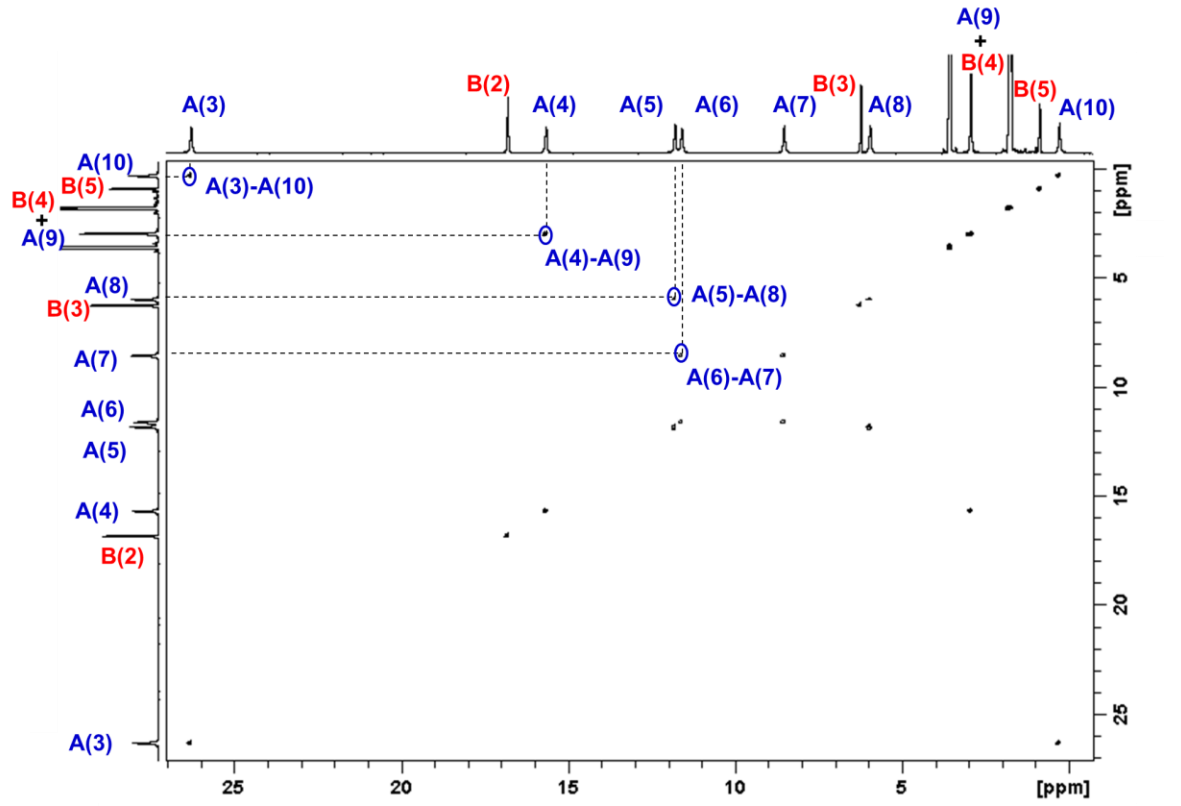

Figure S12. Representative 2D ^{1}H-NMR EXSY experiment of **1–Yb(het)** (19.3 mM; t_{mix} = 5 ms, 300 K; **1–Yb** = 0% ee) taken in THF–d_8.

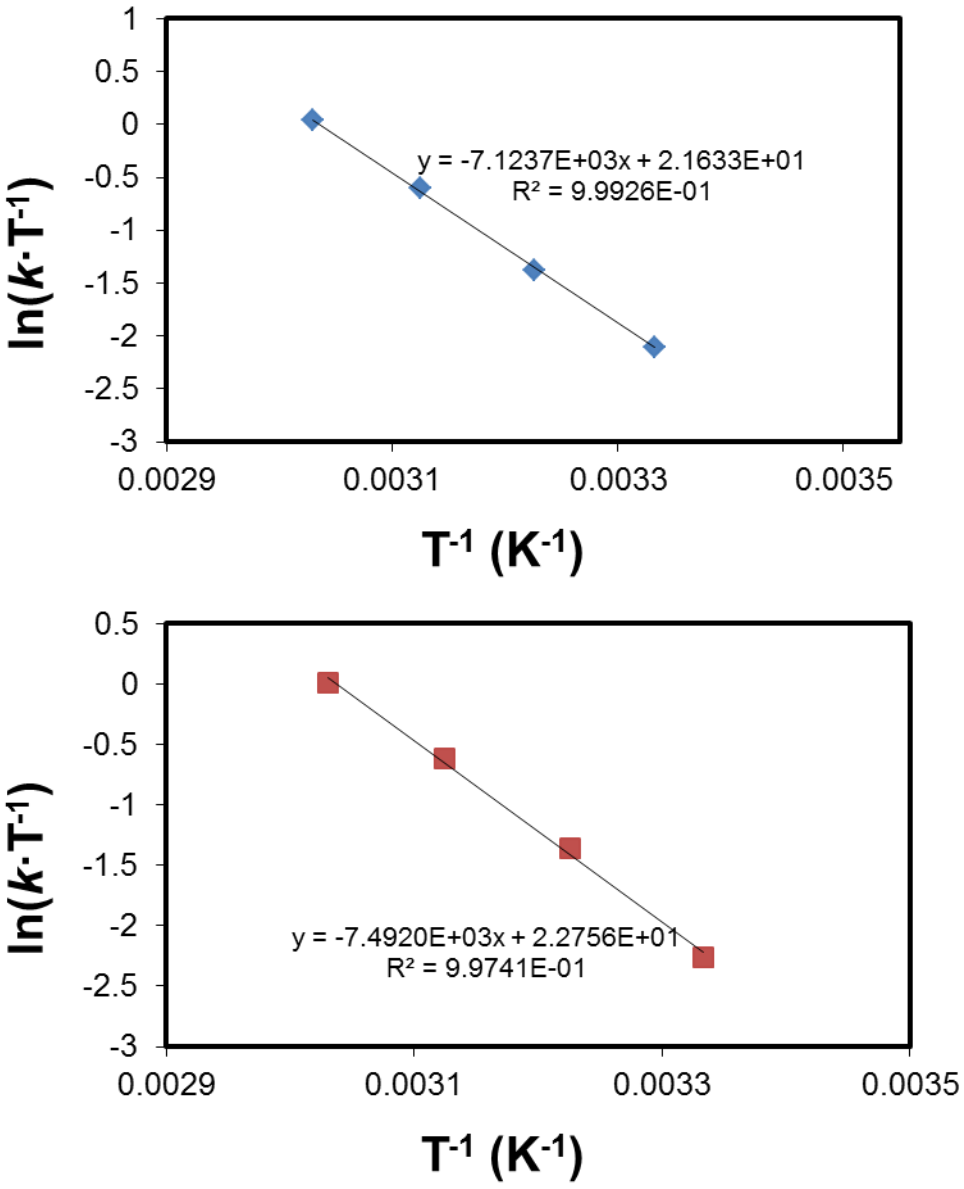

Figure S13. Eyring plots (*top* = A(1) → A(8), *bottom* A(8) → A(1)) obtained from 2D-EXSY ^{1}H-NMR experiments of **1–Yb(het)** (19.3 mM) taken at 300, 310, 320, and 330 K (t_{mix} = 5 ms).

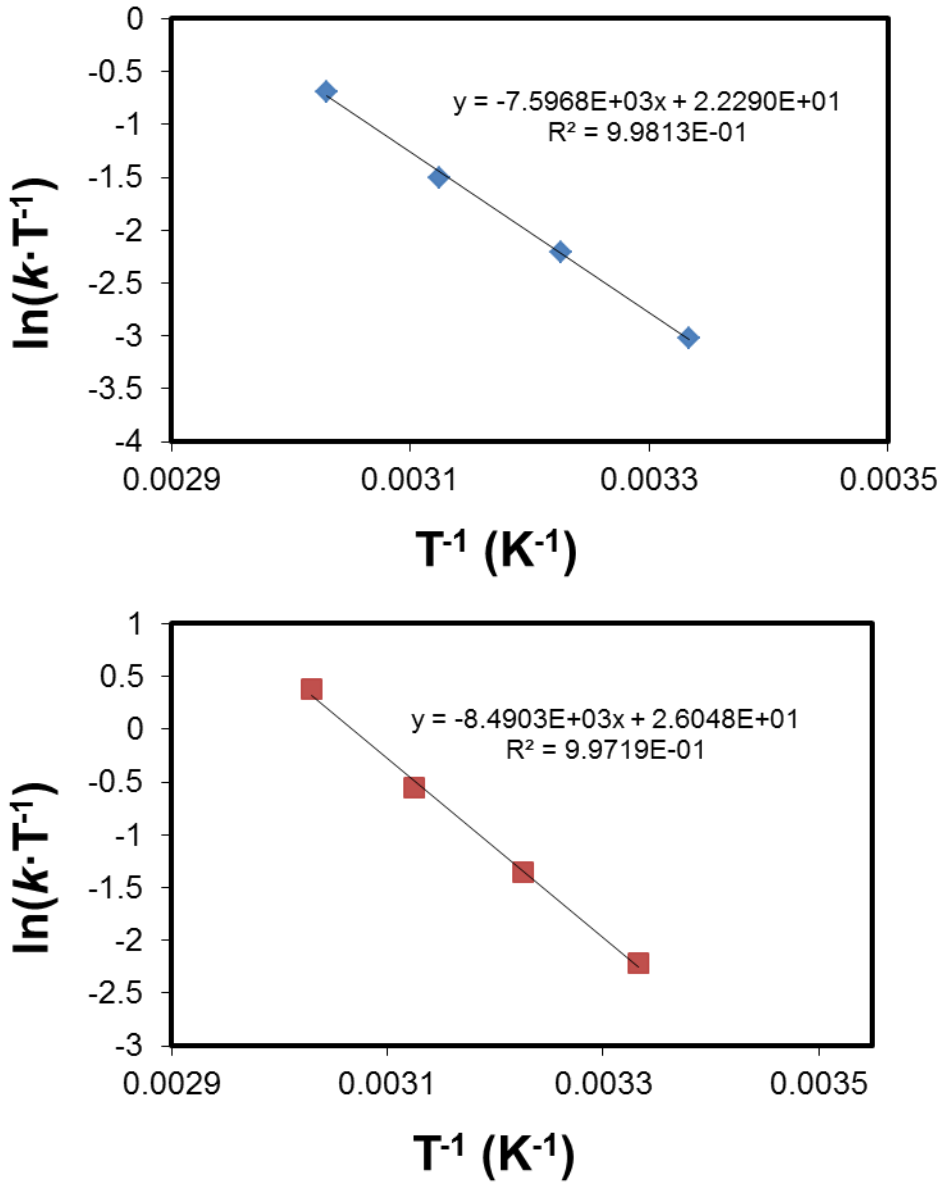

Figure S14. Eyring plots (*top* = Li_A → Li_B, *bottom* Li_B → Li_A) obtained from 2D-EXSY ^{7}Li-NMR experiments of **1–Yb(het)** (19.3 mM) taken at 300, 310, 320, and 330 K (t_{mix} = 5 ms).

Table S1. Diastereomer composition of **1–Ce** (36% ee; 215 – 315 K) determined by ^{7}Li-NMR.

Entry	1-Ce(homo) (%)[a]	1-Ce(het) (%)[a]	Temperature (K)
1	26.8	73.2	215.0
2	26.0	74.0	230.0
3	25.0	75.0	245.0
4	26.7	73.3	260.0
5	25.7	74.3	275.0
6	29.3	70.7	300.0
7	28.8	71.2	315.0

a – Determined by integration of ^{7}Li-NMR resonances of the two diastereomers, **1–Ce(het)** and **1–Ce(homo)**

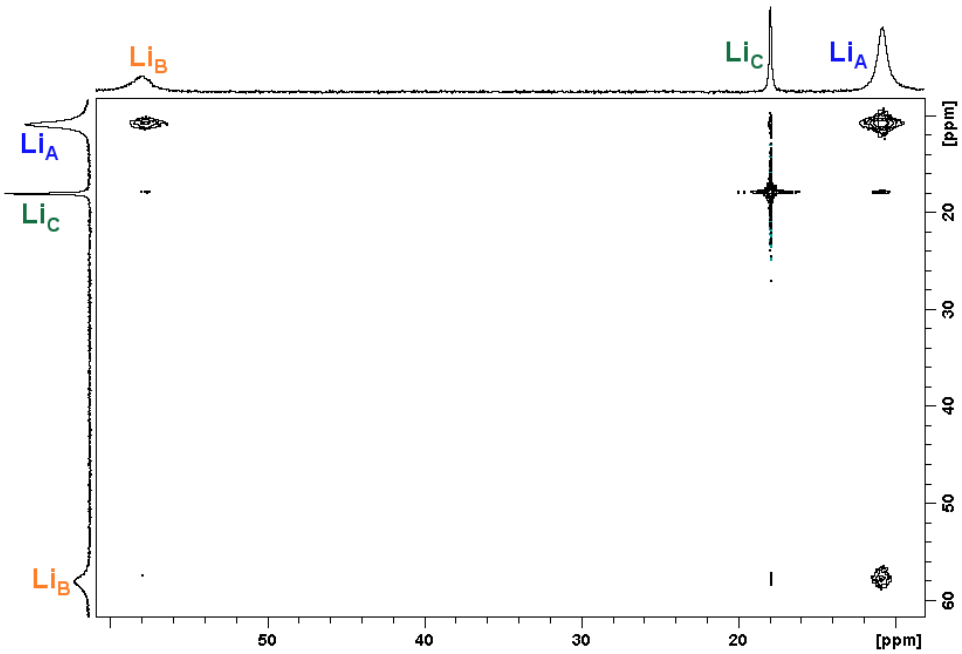

Figure S15. 2D ^{7}Li-NMR EXSY experiment of **1–Ce(het)** / **1–Ce(homo)** ([Ce] = 24.4 mM; t_{mix} = 10 ms, 315 K; **1–Ce** = 0% ee) taken in THF–d_8.

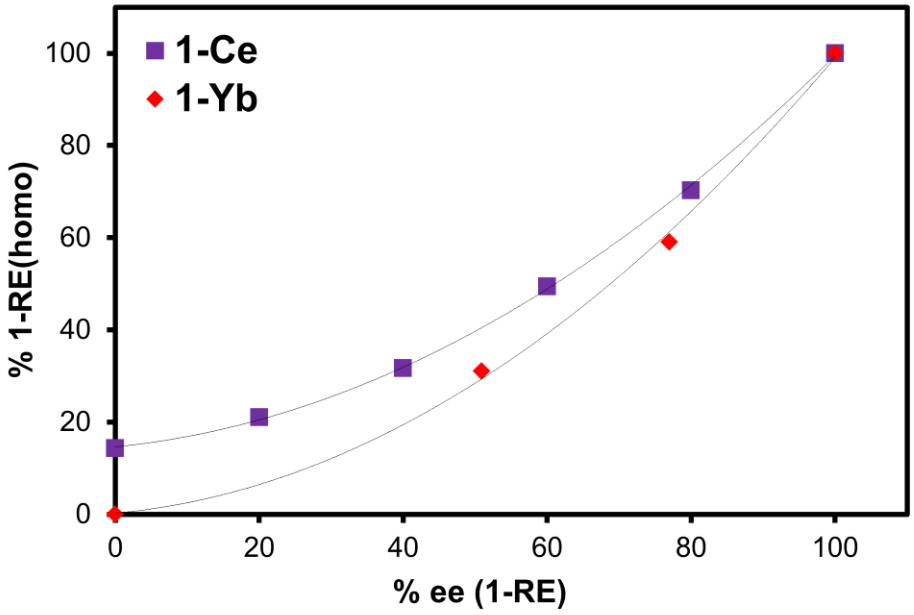

Figure S16. Enantiomeric excess of BINOLate versus percent **1–RE(homo)** in solution (^{7}Li-NMR integration; RE = Ce, Yb). Line provided as a guide for the eye.

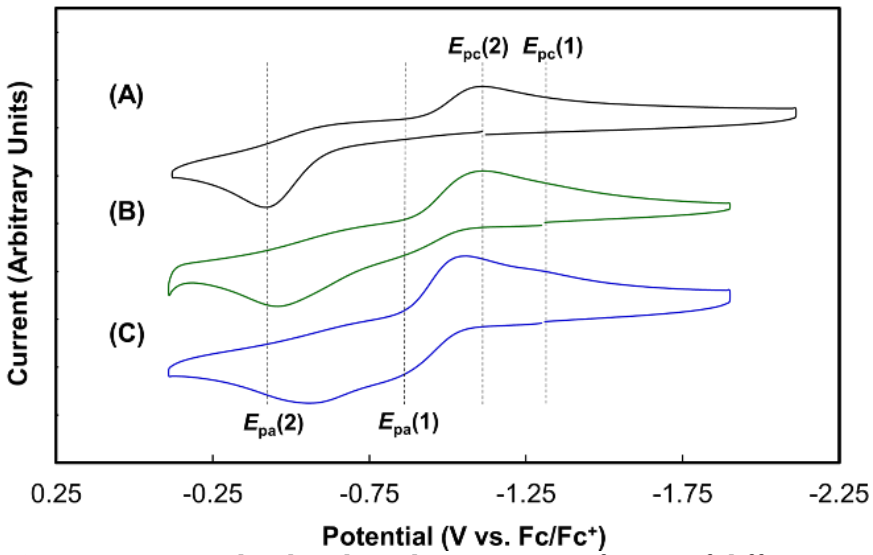

Figure S17. Normalized cyclic voltammograms of **1–Ce** of different optical purities (A) 100% ee (black trace) (B) 50% ee (green trace) (C) 0% ee (blue trace). Cyclic voltammetry performed in THF ([Ce] = ~1 mM; THF, $[NPr_4][BAr^F]$ = 0.100 M, v = 500 mV·s^{-1}). Dashed lines provided as a guide for the eye to identify E_{pa} and E_{pc}.

Table S2. Values of $E_{pa}{}^a$ and $E_{pc}{}^a$ determined for varying optical purity of **1–Ce** in THF.

1–Ce (% ee)	$E_{pa}(1)$ **1–Ce(het)** (V *vs*. Fc)	$E_{pc}(1)$ **1–Ce(het)** (V *vs*. Fc)	$E_{pa}(2)$ **1–Ce(homo)** (V *vs*. Fc)	$E_{pc}(2)$ **1–Ce(homo)** (V *vs*. Fc)
100	---	---	–0.430	–1.110
50	–0.880	–1.360	–0.470	–1.110
0	–0.860	–1.310	–0.585	–1.075

a – v = 500 mV·s^{-1}

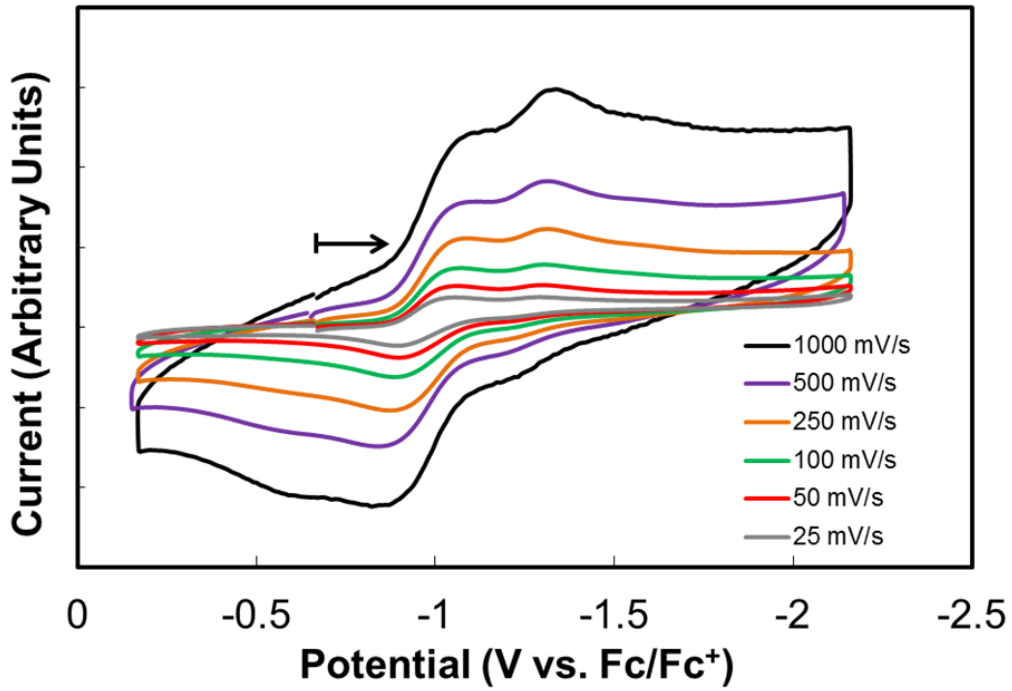

Figure S18. Cyclic voltammogram for $[Li_2(THF)_4][BINOLate)_3Ce]$ (**2–Ce(het)**) (**2–Ce** = 0% ee) collected from – 0.17 to –2.16 V

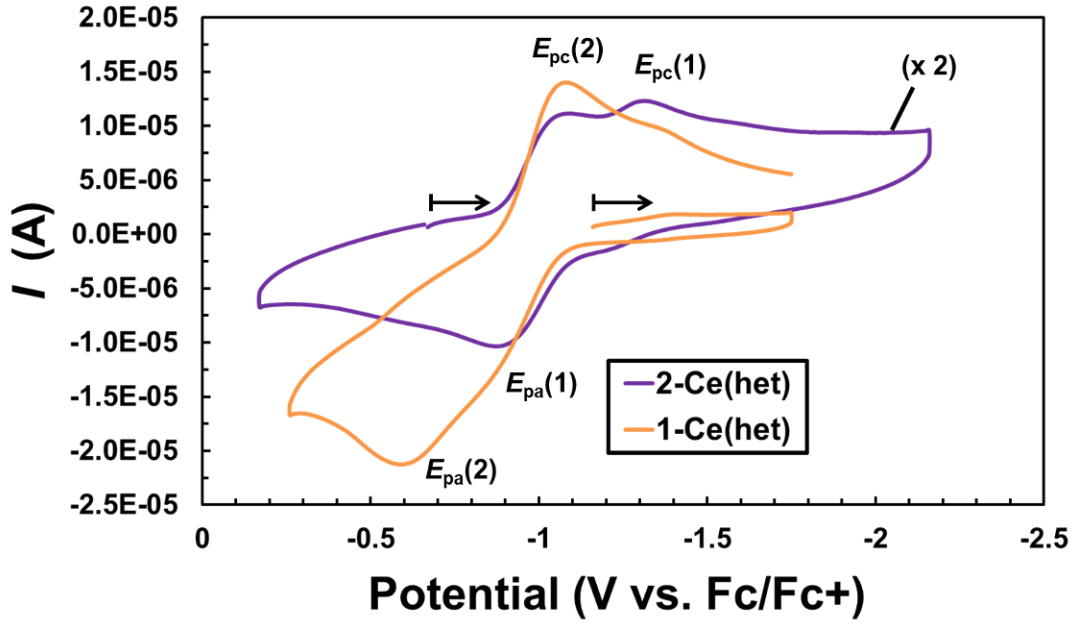

Figure S19. Overlay of cyclic voltammograms for $[Li_2(THF)_4][BINOLate)_3Ce]$ (**2–Ce(het)**) and $[Li_3(THF)_6][(BINOLate)_3Ce]$ (**1–Ce(het)** = 0% ee) collected at 250 $mV \cdot s^{-1}$

Figure S20. Electronic Absorption Spectra of **1–Ce(het)** (black trace) and **2–Ce(het)** (purple trace) in THF.

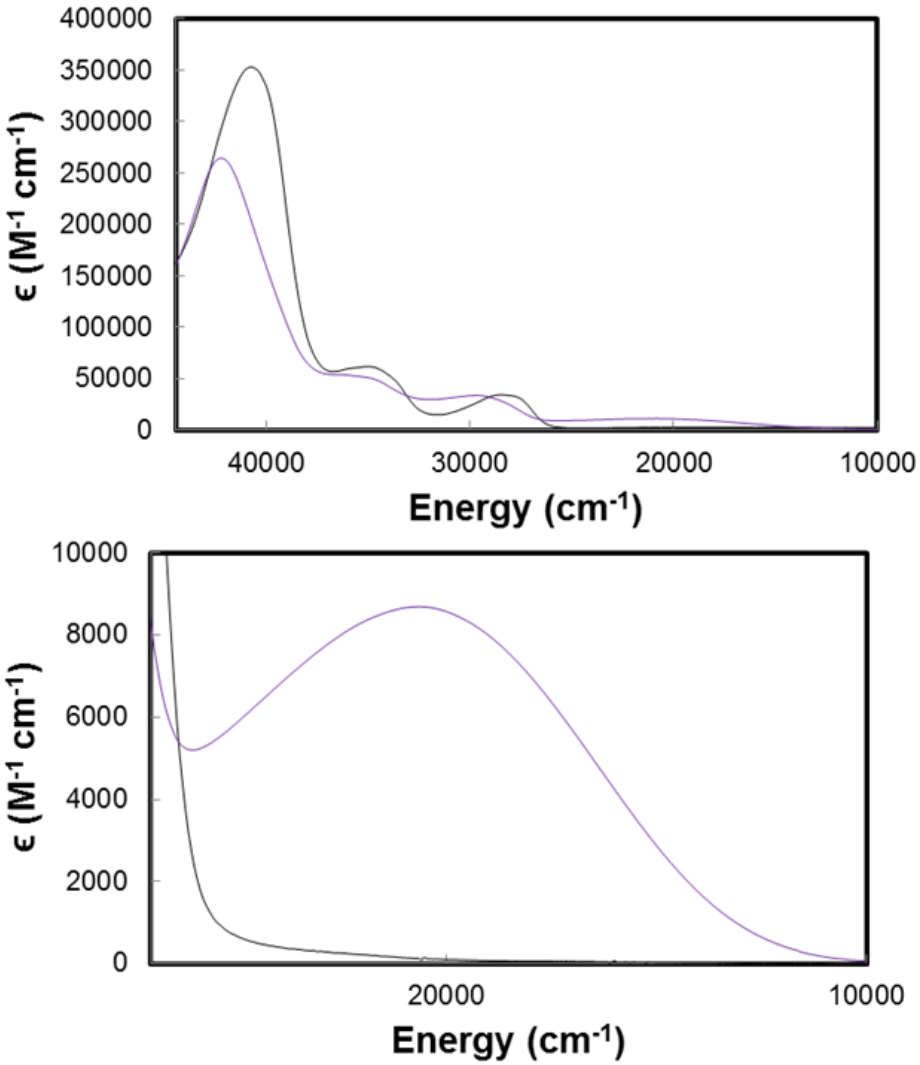

[$Li_3(THF)_6$][$(BINOLate)_3Ce$] (**1–Ce(het)**)

Assignment	**ε (M^{-1} cm^{-1})**	**λ (nm)**	**1/λ (cm^{-1})**
π - π*	3.53E+05	245	4.08E+04
π - π*	6.16E+04	285	3.51E+04
π - π*	3.40E+04	351	2.85E+04

[$Li_2(THF)_4$][$(BINOLate)_3Ce$] (**2–Ce(het)**)

Assignment	**ε (M^{-1} cm^{-1})**	**λ (nm)**	**1/λ (cm^{-1})**
π - π*	2.64E+05	2.37E+02	4.22E+04
π - π*	5.38E+04	2.74E+02	3.65E+04
π - π*	3.35E+04	3.36E+02	2.98E+04
LMCT	8.69E+03	85E+02	2.06E+04

Table S3. Concentration and rate data for the reaction of **1–Ce** with trityl chloride under pseudo-first order conditions.

Entry	$[Ce^{III}]_{Total}$ (mM)	1–Ce(homo) (mM)[a]	1–Ce(het) (mM)[a]	ee (%)[b]	k_{obs} (x 10^{-3} s^{-1})[c]
1	1.26	0.180	1.076	0	0.774
2	1.26	0.264	0.991	20	1.05
3	1.26	0.399	0.857	40	1.61
4	1.26	0.621	0.635	60	2.40
5	1.26	0.882	0.373	80	3.22
6	1.25	1.25	0.000	100	3.83

a – Determined by integration of ^{7}Li resonances of Li_A, Li_B, and Li_C from ^{7}Li-NMR. *b* – Optical purity of BINOL. *c* – Observed rate constant for **1–Ce(het)/1–Ce(homo)** + Ph_3Cl in THF under pseudo-first order conditions (10 equiv Ph_3Cl; $[1–Ce]_{Total}$ = 1.26 mM). Determined following the generation of **2–Ce(het)** during the reaction as measured by UV-Vis spectroscopy (λ = 487 nm).

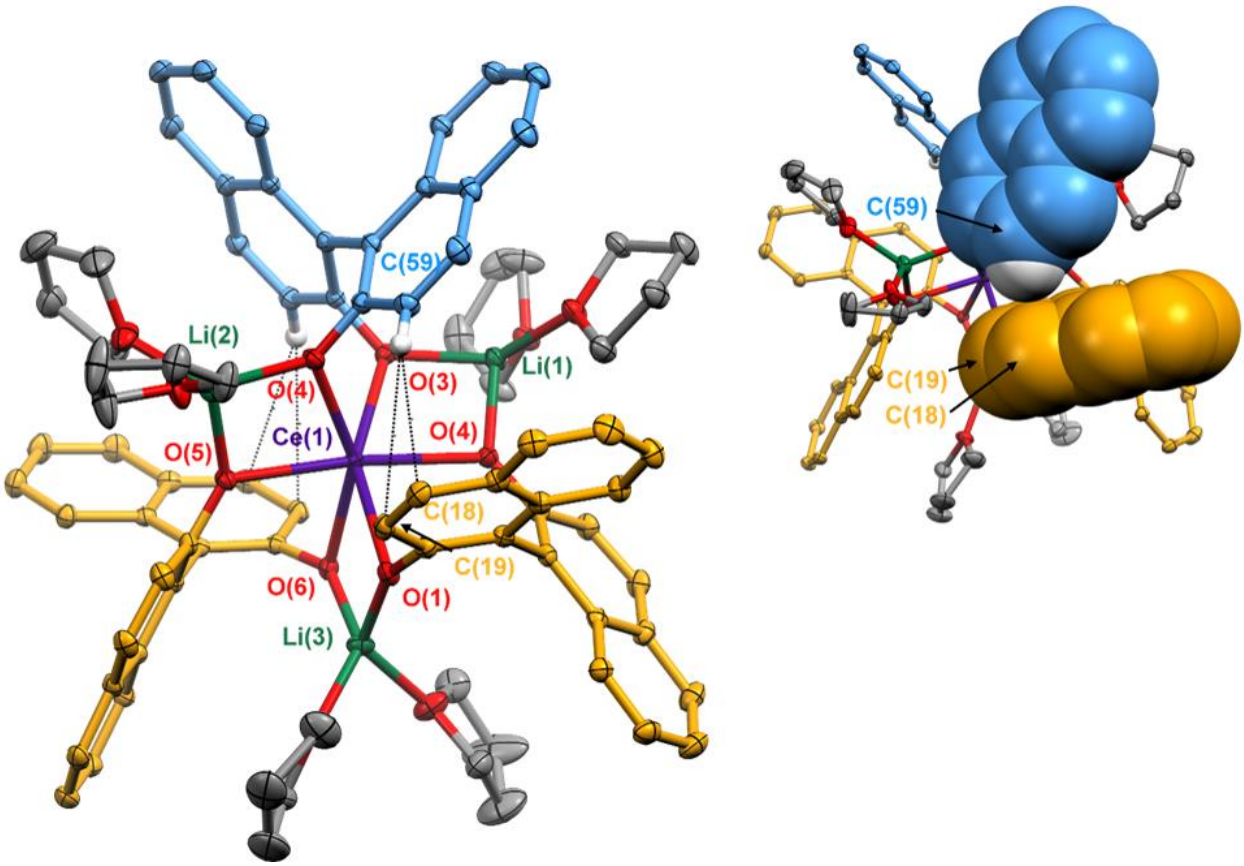

Figure S21. Thermal ellipsoid plot (30% probability) and space-filling model of **1–Ce(het)** highlighting C–H–π interaction in the solid state. The BINOLate ligands have been colored blue and yellow to indicate the *SS*/*RR* and *R*/*S* fragments respectively.

Table S4. Crystallographic parameters for compounds **1–Ce(het)** and **2–Ce(het)**.

	1–Ce(het)·2THF·C_5H_{12}	**2–Ce(het)**
Empirical formula	$C_{97}H_{112}O_{14}Li_3Ce$	$C_{80}H_{76}O_{11}Li_2Ce$
Formula weight	1662.81	1367.41
Temperature (K)	143(1)	143(1)
Wavelength (Å)	0.71073	0.71073
Crystal system	triclinic	monoclinic
Space group	P	$P2_1/c$
Cell constants		
a (Å)	15.6917(12)	15.7715(13)
b (Å)	16.7884(6)	12.9851(11)
c (Å)	18.8233(7)	32.521(3)
α (°)	111.706(2)	90
β (°)	103.016(2)	97.852(5)
γ (°)	97.558(3)	90
V ($Å^3$)	4360.6(4)	6597.7(10)
Z	2	4
ρ_{calc} (mg/cm^3)	1.266	1.377
μ (Mo Kα) (mm^{-1})	0.585	0.754
F(000)	1746	2832
Crystal size (mm^3)	0.35 x 0.25 x 0.08	0.36 x 0.12 x 0.10
Theta range for data collection	1.54 to 27.53°	1.69 to 27.52°
Index ranges	$-20 \le h \le 20$, $-21 \le k \le 21$, $-24 \le l \le 24$	$-20 \le h \le 20$, $-16 \le k \le 16$, $-42 \le l \le 42$
Reflections collected	123592	152011
Independent collections	19902 [R(int) = 0.0247]	15194 [R(int) = 0.0405]
Completeness to theta = 27.52°	99.00%	99.90%
Absorption correction	Semi-empirical from equivalents	Semi-empirical from equivalents
Max and min. transmission	0.7456 and 0.7076	0.7456 and 0.6698
Refinement method	Full-matrix least-squares on F^2	Full-matrix least-squares on F^2
Data / restraints / parameters	19902 / 30 / 1046	15194 / 0 / 822
Goodness–of–fit on F^2	1.046	1.086
Final R indices [I>2sigma(I)]	R1 = 0.0377, wR2 = 0.0990	R1 = 0.0366, wR2 = 0.0912
R indices (all data)	R1 = 0.0463, wR2 = 0.1074	R1 = 0.0475, wR2 = 0.1000
Largest diff. peak and hole ($e \cdot Å^{-3}$)	1.202 and -0.757	1.692 and -0.769

Table S5a. Bond lengths for compound **1**–**Ce(het)** (Å).

Ce1-O5	2.3743(16)	Ce1-O3	2.3900(17)	Ce1-O1	2.3908(16)
Ce1-O6	2.3909(17)	Ce1-O2	2.3924(16)	Ce1-O4	2.3947(16)
Ce1-C20	2.987(2)	Ce1-C21	3.020(2)	Ce1-Li1	3.270(4)
Ce1-Li2	3.290(4)	Ce1-Li3	3.293(4)	O1-C1	1.331(3)
O1-Li3	1.946(4)	O2-C20	1.331(3)	O2-Li1	1.888(5)
O3-C21	1.336(3)	O3-Li1	1.922(4)	O4-C40	1.328(3)
O4-Li2	1.927(5)	O5-C41	1.334(3)	O5-Li3	1.955(4)
O6-C60	1.335(3)	O6-Li2	1.899(5)	O7-C61	1.420(3)
O7-C64	1.431(4)	O7-Li1	1.962(5)	O8-C65	1.411(4)
O8-C68	1.453(4)	O8-Li1	1.957(5)	O9-C69	1.417(4)
O9-C72	1.433(4)	O9-Li2	1.969(5)	O10-C73	1.400(4)
O10-C76	1.425(4)	O10-Li2	1.952(5)	O11-C77	1.440(3)
O11-C80	1.444(3)	O11-Li3	1.947(4)	O12-C84	1.424(4)
O12-C81	1.437(3)	O12-Li3	1.991(5)	C1-C10	1.396(3)
C1-C2	1.428(3)	C2-C3	1.358(4)	C3-C4	1.412(4)
C4-C5	1.416(4)	C4-C9	1.424(3)	C5-C6	1.368(4)
C6-C7	1.396(4)	C7-C8	1.370(4)	C8-C9	1.419(3)
C9-C10	1.428(3)	C10-C11	1.496(3)	C11-C20	1.394(3)
C11-C12	1.432(3)	C12-C13	1.423(3)	C12-C17	1.427(3)
C13-C14	1.369(4)	C14-C15	1.406(4)	C15-C16	1.359(4)
C16-C17	1.414(3)	C17-C18	1.411(4)	C18-C19	1.361(4)
C19-C20	1.426(3)	C21-C30	1.394(3)	C21-C22	1.426(3)
C22-C23	1.363(3)	C23-C24	1.415(3)	C24-C25	1.417(3)
C24-C29	1.425(3)	C25-C26	1.363(4)	C26-C27	1.409(4)
C27-C28	1.370(3)	C28-C29	1.425(3)	C29-C30	1.429(3)
C30-C31	1.491(3)	C31-C40	1.395(3)	C31-C32	1.426(3)
C32-C33	1.420(3)	C32-C37	1.425(3)	C33-C34	1.370(3)
C34-C35	1.409(4)	C35-C36	1.362(4)	C36-C37	1.417(3)
C37-C38	1.415(4)	C38-C39	1.359(4)	C39-C40	1.428(3)
C41-C50	1.392(3)	C41-C42	1.426(3)	C42-C43	1.362(3)
C43-C44	1.414(4)	C44-C49	1.423(3)	C44-C45	1.427(3)
C45-C46	1.365(4)	C46-C47	1.397(4)	C47-C48	1.373(4)
C48-C49	1.423(3)	C49-C50	1.429(3)	C50-C51	1.490(3)
C51-C60	1.397(3)	C51-C52	1.430(3)	C52-C53	1.423(3)
C52-C57	1.427(4)	C53-C54	1.368(4)	C54-C55	1.406(4)
C55-C56	1.361(4)	C56-C57	1.419(4)	C57-C58	1.413(4)
C58-C59	1.362(4)	C59-C60	1.425(3)	C61-C62	1.489(6)
C62-C63	1.468(7)	C63-C64	1.476(6)	C65-C66	1.513(7)
C65-C66'	1.536(12)	C66-C67	1.536(9)	C66'-C67	1.432(13)
C67-C68	1.505(6)	C69-C70	1.509(4)	C70-C71	1.494(6)
C71-C72	1.456(7)	C73-C74	1.513(4)	C74-C75	1.508(5)
C75-C76	1.404(6)	C77-C78	1.506(4)	C78-C79	1.511(4)
C79-C80	1.518(4)	C81-C82	1.490(5)	C82-C83	1.497(6)
C83-C84	1.521(4)	O13-C88	1.383(5)	O13-C85	1.389(5)

C85-C86	1.459(6)	C86-C87	1.491(6)	C87-C88	1.472(6)
O14-C89	1.425(10)	O14-C92	1.447(11)	C89-C90	1.491(8)
C90-C91	1.429(10)	C91-C92	1.480(11)	C93-C94	1.593(11)
C94-C95	1.389(10)	C95-C96	1.523(9)	C96-C97	1.638(11)

Table S5b. Bond angles for compound **1–Ce(het)** (°).

O5-Ce1-O3	110.55(6)	O5-Ce1-O1	71.21(5)	O3-Ce1-O1	97.83(5)
O5-Ce1-O6	78.71(5)	O3-Ce1-O6	150.93(5)	O1-Ce1-O6	111.20(6)
O5-Ce1-O2	151.64(6)	O3-Ce1-O2	70.38(5)	O1-Ce1-O2	80.53(5)
O6-Ce1-O2	114.86(6)	O5-Ce1-O4	118.45(6)	O3-Ce1-O4	81.70(5)
O1-Ce1-O4	169.94(5)	O6-Ce1-O4	70.01(5)	O2-Ce1-O4	89.89(6)
O5-Ce1-C20	136.98(6)	O3-Ce1-C20	95.76(6)	O1-Ce1-C20	71.98(6)
O6-Ce1-C20	94.70(6)	O2-Ce1-C20	25.75(6)	O4-Ce1-C20	98.03(6)
O5-Ce1-C21	94.69(6)	O3-Ce1-C21	25.34(5)	O1-Ce1-C21	112.14(6)
O6-Ce1-C21	131.05(6)	O2-Ce1-C21	93.75(6)	O4-Ce1-C21	71.33(6)
C20-Ce1-C21	119.50(6)	O5-Ce1-Li1	139.41(9)	O3-Ce1-Li1	35.60(8)
O1-Ce1-Li1	89.24(9)	O6-Ce1-Li1	141.83(9)	O2-Ce1-Li1	34.78(8)
O4-Ce1-Li1	84.57(9)	C20-Ce1-Li1	60.30(9)	C21-Ce1-Li1	59.47(9)
O5-Ce1-Li2	98.32(10)	O3-Ce1-Li2	116.58(9)	O1-Ce1-Li2	145.38(9)
O6-Ce1-Li2	34.68(9)	O2-Ce1-Li2	106.46(10)	O4-Ce1-Li2	35.40(9)
C20-Ce1-Li2	99.40(10)	C21-Ce1-Li2	101.35(9)	Li1-Ce1-Li2	116.14(12)
O5-Ce1-Li3	35.94(8)	O3-Ce1-Li3	111.88(8)	O1-Ce1-Li3	35.78(8)
O6-Ce1-Li3	91.90(8)	O2-Ce1-Li3	116.14(8)	O4-Ce1-Li3	153.19(8)
C20-Ce1-Li3	103.19(8)	C21-Ce1-Li3	110.78(8)	Li1-Ce1-Li3	120.22(11)
Li2-Ce1-Li3	123.38(11)	C1-O1-Li3	130.21(19)	C1-O1-Ce1	129.97(13)
Li3-O1-Ce1	98.31(14)	C20-O2-Li1	156.2(2)	C20-O2-Ce1	102.92(13)
Li1-O2-Ce1	98.94(14)	C21-O3-Li1	146.8(2)	C21-O3-Ce1	104.73(13)
Li1-O3-Ce1	98.03(14)	C40-O4-Li2	133.0(2)	C40-O4-Ce1	125.74(14)
Li2-O4-Ce1	98.58(15)	C41-O5-Li3	134.78(19)	C41-O5-Ce1	119.92(13)
Li3-O5-Ce1	98.60(14)	C60-O6-Li2	142.8(2)	C60-O6-Ce1	117.03(13)
Li2-O6-Ce1	99.55(15)	C61-O7-C64	108.5(2)	C61-O7-Li1	128.0(2)
C64-O7-Li1	122.1(2)	C65-O8-C68	110.0(3)	C65-O8-Li1	121.4(2)
C68-O8-Li1	128.1(2)	C69-O9-C72	107.6(3)	C69-O9-Li2	116.0(2)
C72-O9-Li2	128.0(3)	C73-O10-C76	107.0(3)	C73-O10-Li2	126.2(2)
C76-O10-Li2	126.4(3)	C77-O11-C80	109.9(2)	C77-O11-Li3	119.73(19)
C80-O11-Li3	130.0(2)	C84-O12-C81	109.3(2)	C84-O12-Li3	116.4(2)
C81-O12-Li3	118.1(2)	O1-C1-C10	122.8(2)	O1-C1-C2	118.6(2)
C10-C1-C2	118.6(2)	C3-C2-C1	121.7(2)	C2-C3-C4	121.0(2)
C3-C4-C5	122.4(2)	C3-C4-C9	118.5(2)	C5-C4-C9	119.1(2)
C6-C5-C4	121.2(3)	C5-C6-C7	119.9(3)	C8-C7-C6	120.7(3)
C7-C8-C9	121.3(2)	C8-C9-C4	117.9(2)	C8-C9-C10	122.1(2)
C4-C9-C10	120.0(2)	C1-C10-C9	119.7(2)	C1-C10-C11	120.2(2)
C9-C10-C11	120.1(2)	C20-C11-C12	119.3(2)	C20-C11-C10	120.11(19)
C12-C11-C10	120.5(2)	C13-C12-C17	117.5(2)	C13-C12-C11	122.6(2)
C17-C12-C11	119.9(2)	C14-C13-C12	121.3(2)	C13-C14-C15	120.5(3)

C16-C15-C14	119.7(2)	C15-C16-C17	121.6(2)	C18-C17-C16	121.7(2)
C18-C17-C12	119.0(2)	C16-C17-C12	119.2(2)	C19-C18-C17	120.8(2)
C18-C19-C20	121.4(2)	O2-C20-C11	121.5(2)	O2-C20-C19	118.7(2)
C11-C20-C19	119.6(2)	O2-C20-Ce1	51.33(10)	C11-C20-Ce1	108.89(14)
C19-C20-Ce1	104.89(15)	O3-C21-C30	122.01(19)	O3-C21-C22	118.7(2)
C30-C21-C22	119.2(2)	O3-C21-Ce1	49.93(10)	C30-C21-Ce1	107.96(14)
C22-C21-Ce1	108.18(14)	C23-C22-C21	121.5(2)	C22-C23-C24	121.0(2)
C23-C24-C25	122.1(2)	C23-C24-C29	118.4(2)	C25-C24-C29	119.5(2)
C26-C25-C24	121.1(2)	C25-C26-C27	120.0(2)	C28-C27-C26	120.5(2)
C27-C28-C29	121.2(2)	C28-C29-C24	117.7(2)	C28-C29-C30	121.9(2)
C24-C29-C30	120.3(2)	C21-C30-C29	119.6(2)	C21-C30-C31	119.83(19)
C29-C30-C31	120.59(19)	C40-C31-C32	119.7(2)	C40-C31-C30	119.82(19)
C32-C31-C30	120.52(19)	C33-C32-C37	117.5(2)	C33-C32-C31	122.3(2)
C37-C32-C31	120.2(2)	C34-C33-C32	121.3(2)	C33-C34-C35	120.9(2)
C36-C35-C34	119.2(2)	C35-C36-C37	121.6(2)	C38-C37-C36	122.0(2)
C38-C37-C32	118.6(2)	C36-C37-C32	119.4(2)	C39-C38-C37	120.9(2)
C38-C39-C40	121.6(2)	O4-C40-C31	122.2(2)	O4-C40-C39	118.7(2)
C31-C40-C39	119.1(2)	O5-C41-C50	122.3(2)	O5-C41-C42	118.4(2)
C50-C41-C42	119.3(2)	C43-C42-C41	121.5(2)	C42-C43-C44	120.8(2)
C43-C44-C49	118.6(2)	C43-C44-C45	121.9(2)	C49-C44-C45	119.5(2)
C46-C45-C44	121.0(3)	C45-C46-C47	119.8(2)	C48-C47-C46	121.1(3)
C47-C48-C49	121.2(3)	C44-C49-C48	117.5(2)	C44-C49-C50	120.2(2)
C48-C49-C50	122.3(2)	C41-C50-C49	119.5(2)	C41-C50-C51	119.3(2)
C49-C50-C51	121.2(2)	C60-C51-C52	119.1(2)	C60-C51-C50	119.5(2)
C52-C51-C50	121.4(2)	C53-C52-C57	117.5(2)	C53-C52-C51	122.1(2)
C57-C52-C51	120.4(2)	C54-C53-C52	121.3(2)	C53-C54-C55	120.9(3)
C56-C55-C54	119.6(3)	C55-C56-C57	121.4(3)	C58-C57-C56	122.0(3)
C58-C57-C52	118.6(2)	C56-C57-C52	119.3(2)	C59-C58-C57	120.7(2)
C58-C59-C60	121.7(2)	O6-C60-C51	122.3(2)	O6-C60-C59	118.2(2)
C51-C60-C59	119.4(2)	O7-C61-C62	105.2(3)	C63-C62-C61	104.4(4)
C62-C63-C64	107.8(4)	O7-C64-C63	105.5(3)	O8-C65-C66	107.4(4)
O8-C65-C66'	102.4(7)	C66-C65-C66'	40.0(6)	C65-C66-C67	101.1(5)
C67-C66'-C65	104.9(7)	C66'-C67-C68	103.6(6)	C66'-C67-C66	41.0(7)
C68-C67-C66	104.7(4)	O8-C68-C67	106.0(4)	O9-C69-C70	106.9(3)
C71-C70-C69	105.5(3)	C72-C71-C70	105.9(3)	O9-C72-C71	107.8(3)
O10-C73-C74	107.3(2)	C75-C74-C73	103.5(3)	C76-C75-C74	105.9(3)
C75-C76-O10	107.9(3)	O11-C77-C78	106.6(2)	C77-C78-C79	102.4(2)
C78-C79-C80	104.0(2)	O11-C80-C79	105.5(2)	O12-C81-C82	106.5(3)
C81-C82-C83	102.8(3)	C82-C83-C84	102.3(3)	O12-C84-C83	106.0(3)
O2-Li1-O3	92.65(19)	O2-Li1-O8	103.9(2)	O3-Li1-O8	138.3(3)
O2-Li1-O7	125.2(3)	O3-Li1-O7	103.7(2)	O8-Li1-O7	97.4(2)
O2-Li1-Ce1	46.28(10)	O3-Li1-Ce1	46.37(10)	O8-Li1-Ce1	135.2(2)
O7-Li1-Ce1	126.6(2)	O6-Li2-O4	91.7(2)	O6-Li2-O10	113.3(2)
O4-Li2-O10	122.5(3)	O6-Li2-O9	124.9(3)	O4-Li2-O9	105.3(2)

O10-Li2-O9	100.7(2)	O6-Li2-Ce1	45.77(11)	O4-Li2-Ce1	46.02(11)
O10-Li2-Ce1	134.5(2)	O9-Li2-Ce1	124.6(2)	O1-Li3-O11	100.9(2)
O1-Li3-O5	90.67(18)	O11-Li3-O5	137.8(2)	O1-Li3-O12	127.1(2)
O11-Li3-O12	103.3(2)	O5-Li3-O12	101.3(2)	O1-Li3-Ce1	45.91(10)
O11-Li3-Ce1	125.97(18)	O5-Li3-Ce1	45.47(10)	O12-Li3-Ce1	130.58(18)
C88-O13-C85	109.8(3)	O13-C85-C86	108.3(4)	C85-C86-C87	106.0(4)
C88-C87-C86	103.2(4)	O13-C88-C87	108.4(4)	C89-O14-C92	97.1(7)
O14-C89-C90	106.1(7)	C91-C90-C89	107.8(7)	C90-C91-C92	99.9(9)
O14-C92-C91	107.9(9)	C95-C94-C93	116.0(8)	C94-C95-C96	121.4(8)
C95-C96-C97	119.2(7)				

Table S6a. Bond lengths for compound **2–Ce(het)** (Å).

Ce1-O5	2.1755(18)	Ce1-O2	2.1958(18)	Ce1-O1	2.2685(17)
Ce1-O3	2.2709(18)	Ce1-O4	2.2773(17)	Ce1-O6	2.2917(17)
Ce1-C1	2.921(2)	Ce1-C60	3.004(2)	Ce1-Li2	3.204(4)
Ce1-Li1	3.231(4)	O1-C1	1.351(3)	O1-Li1	1.921(5)
O2-C20	1.338(3)	O3-C21	1.351(3)	O3-Li1	1.954(5)
O4-C40	1.349(3)	O4-Li2	1.960(5)	O5-C41	1.339(3)
O6-C60	1.349(3)	O6-Li2	1.913(5)	O7-C64	1.414(4)
O7-C61	1.437(4)	O7-Li1	1.919(5)	O8-C65	1.418(4)
O8-C68	1.420(4)	O8-Li1	1.950(5)	O9-C72	1.437(3)
O9-C69	1.443(3)	O9-Li2	1.947(5)	O10-C73	1.434(4)
O10-C76	1.460(4)	O10-Li2	1.926(5)	O11-C77	1.531(11)
O11-C80	1.573(11)	C1-C10	1.388(3)	C1-C2	1.417(3)
C2-C3	1.359(4)	C3-C4	1.409(4)	C4-C5	1.417(4)
C4-C9	1.427(3)	C5-C6	1.357(4)	C6-C7	1.411(4)
C7-C8	1.365(4)	C8-C9	1.418(3)	C9-C10	1.432(3)
C10-C11	1.484(3)	C11-C20	1.393(3)	C11-C12	1.432(4)
C12-C13	1.420(4)	C12-C17	1.426(4)	C13-C14	1.368(4)
C14-C15	1.405(6)	C15-C16	1.361(6)	C16-C17	1.415(5)
C17-C18	1.411(5)	C18-C19	1.350(4)	C19-C20	1.424(3)
C21-C30	1.384(3)	C21-C22	1.421(4)	C22-C23	1.357(4)
C23-C24	1.416(4)	C24-C25	1.415(4)	C24-C29	1.429(4)
C25-C26	1.363(5)	C26-C27	1.402(5)	C27-C28	1.375(4)
C28-C29	1.417(4)	C29-C30	1.431(3)	C30-C31	1.491(3)
C31-C40	1.387(3)	C31-C32	1.436(3)	C32-C37	1.415(4)
C32-C33	1.425(4)	C33-C34	1.367(4)	C34-C35	1.390(5)
C35-C36	1.367(5)	C36-C37	1.421(4)	C37-C38	1.420(4)
C38-C39	1.357(4)	C39-C40	1.420(4)	C41-C50	1.385(3)
C41-C42	1.422(3)	C42-C43	1.359(4)	C43-C44	1.408(4)
C44-C45	1.421(4)	C44-C49	1.429(4)	C45-C46	1.358(5)
C46-C47	1.411(5)	C47-C48	1.374(4)	C48-C49	1.417(4)
C49-C50	1.431(3)	C50-C51	1.494(3)	C51-C60	1.387(3)
C51-C52	1.433(3)	C52-C53	1.421(4)	C52-C57	1.422(4)
C53-C54	1.374(4)	C54-C55	1.396(5)	C55-C56	1.371(5)

C56-C57	1.420(4)	C57-C58	1.415(4)	C58-C59	1.359(4)
C59-C60	1.425(3)	C61-C62	1.521(4)	C62-C63	1.433(6)
C63-C64	1.501(7)	C65-C66	1.509(5)	C66-C67	1.478(6)
C67-C68	1.462(5)	C69-C70	1.530(4)	C70-C71	1.525(5)
C71-C72	1.502(4)	C73-C74	1.490(6)	C74-C75	1.412(8)
C75-C76	1.507(7)	C77-C78	1.317(13)	C78-C79	1.382(15)
C79-C80	1.410(14)				

Table S6b. Bond angles for compound **2–Ce(het)** (°).

O5-Ce1-O2	150.75(7)	O5-Ce1-O1	92.44(7)	O2-Ce1-O1	78.71(6)
O5-Ce1-O3	91.73(7)	O2-Ce1-O3	111.27(7)	O1-Ce1-O3	71.74(6)
O5-Ce1-O4	111.62(7)	O2-Ce1-O4	90.44(7)	O1-Ce1-O4	143.94(6)
O3-Ce1-O4	80.75(6)	O5-Ce1-O6	81.00(6)	O2-Ce1-O6	87.85(7)
O1-Ce1-O6	139.59(6)	O3-Ce1-O6	147.65(6)	O4-Ce1-O6	72.98(6)
O5-Ce1-C1	88.51(7)	O2-Ce1-C1	71.08(7)	O1-Ce1-C1	26.57(7)
O3-Ce1-C1	98.12(6)	O4-Ce1-C1	159.84(7)	O6-Ce1-C1	113.04(7)
O5-Ce1-C60	70.99(6)	O2-Ce1-C60	87.56(7)	O1-Ce1-C60	115.33(6)
O3-Ce1-C60	161.10(6)	O4-Ce1-C60	98.20(6)	O6-Ce1-C60	25.22(6)
C1-Ce1-C60	89.24(7)	O5-Ce1-Li2	101.12(9)	O2-Ce1-Li2	84.67(9)
O1-Ce1-Li2	163.23(9)	O3-Ce1-Li2	117.17(9)	O4-Ce1-Li2	37.27(9)
O6-Ce1-Li2	36.14(9)	C1-Ce1-Li2	142.79(9)	C60-Ce1-Li2	61.23(9)
O5-Ce1-Li1	97.77(9)	O2-Ce1-Li1	91.15(10)	O1-Ce1-Li1	35.77(9)
O3-Ce1-Li1	36.62(9)	O4-Ce1-Li1	111.61(9)	O6-Ce1-Li1	175.31(9)
C1-Ce1-Li1	62.34(10)	C60-Ce1-Li1	150.17(9)	Li2-Ce1-Li1	148.28(12)
C1-O1-Li1	154.6(2)	C1-O1-Ce1	104.75(14)	Li1-O1-Ce1	100.58(15)
C20-O2-Ce1	134.96(15)	C21-O3-Li1	137.1(2)	C21-O3-Ce1	117.88(14)
Li1-O3-Ce1	99.50(16)	C40-O4-Li2	130.1(2)	C40-O4-Ce1	123.91(15)
Li2-O4-Ce1	98.00(15)	C41-O5-Ce1	132.01(15)	C60-O6-Li2	151.7(2)
C60-O6-Ce1	108.42(14)	Li2-O6-Ce1	98.91(15)	C64-O7-C61	108.6(3)
C64-O7-Li1	121.0(3)	C61-O7-Li1	116.7(2)	C65-O8-C68	110.0(2)
C65-O8-Li1	130.1(2)	C68-O8-Li1	118.2(2)	C72-O9-C69	105.4(2)
C72-O9-Li2	131.7(2)	C69-O9-Li2	122.5(2)	C73-O10-C76	107.9(3)
C73-O10-Li2	117.4(2)	C76-O10-Li2	118.4(2)	C77-O11-C80	98.6(7)
O1-C1-C10	121.3(2)	O1-C1-C2	117.9(2)	C10-C1-C2	120.7(2)
O1-C1-Ce1	48.68(11)	C10-C1-Ce1	111.16(15)	C2-C1-Ce1	104.90(16)
C3-C2-C1	120.6(2)	C2-C3-C4	121.1(2)	C3-C4-C5	121.5(2)
C3-C4-C9	119.0(2)	C5-C4-C9	119.5(2)	C6-C5-C4	121.2(3)
C5-C6-C7	119.6(3)	C8-C7-C6	120.7(2)	C7-C8-C9	121.5(2)
C8-C9-C4	117.4(2)	C8-C9-C10	122.9(2)	C4-C9-C10	119.6(2)
C1-C10-C9	118.9(2)	C1-C10-C11	119.5(2)	C9-C10-C11	121.5(2)
C20-C11-C12	118.9(2)	C20-C11-C10	119.5(2)	C12-C11-C10	121.5(2)
C13-C12-C17	117.9(3)	C13-C12-C11	122.0(2)	C17-C12-C11	120.1(3)
C14-C13-C12	121.4(3)	C13-C14-C15	120.3(4)	C16-C15-C14	119.9(3)
C15-C16-C17	121.6(3)	C18-C17-C16	122.6(3)	C18-C17-C12	118.4(3)
C16-C17-C12	118.9(3)	C19-C18-C17	121.4(3)	C18-C19-C20	121.2(3)

O2-C20-C11	122.0(2)	O2-C20-C19	118.2(2)	C11-C20-C19	119.8(2)
O3-C21-C30	121.3(2)	O3-C21-C22	118.5(2)	C30-C21-C22	120.2(2)
C23-C22-C21	121.2(2)	C22-C23-C24	120.9(2)	C25-C24-C23	121.8(3)
C25-C24-C29	119.5(3)	C23-C24-C29	118.6(2)	C26-C25-C24	121.1(3)
C25-C26-C27	119.8(3)	C28-C27-C26	120.7(3)	C27-C28-C29	121.2(3)
C28-C29-C24	117.6(2)	C28-C29-C30	122.5(2)	C24-C29-C30	119.9(2)
C21-C30-C29	119.2(2)	C21-C30-C31	120.0(2)	C29-C30-C31	120.8(2)
C40-C31-C32	119.1(2)	C40-C31-C30	120.7(2)	C32-C31-C30	120.1(2)
C37-C32-C33	117.8(2)	C37-C32-C31	120.1(2)	C33-C32-C31	122.0(2)
C34-C33-C32	121.2(3)	C33-C34-C35	120.9(3)	C36-C35-C34	119.8(3)
C35-C36-C37	121.1(3)	C32-C37-C38	118.6(3)	C32-C37-C36	119.2(3)
C38-C37-C36	122.2(3)	C39-C38-C37	120.9(3)	C38-C39-C40	121.2(3)
O4-C40-C31	122.1(2)	O4-C40-C39	118.1(2)	C31-C40-C39	119.9(2)
O5-C41-C50	121.9(2)	O5-C41-C42	118.3(2)	C50-C41-C42	119.8(2)
C43-C42-C41	121.3(3)	C42-C43-C44	120.8(2)	C43-C44-C45	121.8(3)
C43-C44-C49	119.0(2)	C45-C44-C49	119.2(3)	C46-C45-C44	121.4(3)
C45-C46-C47	119.7(3)	C48-C47-C46	120.6(3)	C47-C48-C49	121.2(3)
C48-C49-C44	117.9(2)	C48-C49-C50	122.5(2)	C44-C49-C50	119.5(2)
C41-C50-C49	119.5(2)	C41-C50-C51	119.8(2)	C49-C50-C51	120.7(2)
C60-C51-C52	119.0(2)	C60-C51-C50	120.1(2)	C52-C51-C50	120.9(2)
C53-C52-C57	117.9(2)	C53-C52-C51	122.1(2)	C57-C52-C51	120.0(2)
C54-C53-C52	120.9(3)	C53-C54-C55	120.8(3)	C56-C55-C54	120.3(3)
C55-C56-C57	120.4(3)	C58-C57-C56	121.2(3)	C58-C57-C52	119.1(2)
C56-C57-C52	119.7(3)	C59-C58-C57	120.5(2)	C58-C59-C60	121.2(2)
O6-C60-C51	121.3(2)	O6-C60-C59	118.5(2)	C51-C60-C59	120.2(2)
O6-C60-Ce1	46.36(10)	C51-C60-Ce1	108.50(15)	C59-C60-Ce1	110.67(16)
O7-C61-C62	105.3(3)	C63-C62-C61	103.7(3)	C62-C63-C64	107.6(4)
O7-C64-C63	106.9(3)	O8-C65-C66	106.4(3)	C67-C66-C65	105.6(3)
C68-C67-C66	105.5(3)	O8-C68-C67	108.8(3)	O9-C69-C70	105.2(2)
C71-C70-C69	104.2(2)	C72-C71-C70	104.7(3)	O9-C72-C71	104.5(2)
O10-C73-C74	108.0(3)	C75-C74-C73	104.6(4)	C74-C75-C76	106.9(4)
O10-C76-C75	104.2(4)	C78-C77-O11	104.5(9)	C77-C78-C79	122.6(12)
C78-C79-C80	100.0(12)	C79-C80-O11	111.8(10)	O7-Li1-O1	104.4(2)
O7-Li1-O8	113.6(2)	O1-Li1-O8	119.9(3)	O7-Li1-O3	125.7(3)
O1-Li1-O3	86.7(2)	O8-Li1-O3	105.0(2)	O7-Li1-Ce1	131.3(2)
O1-Li1-Ce1	43.64(11)	O8-Li1-Ce1	114.68(19)	O3-Li1-Ce1	43.89(11)
O6-Li2-O10	118.9(2)	O6-Li2-O9	112.0(2)	O10-Li2-O9	110.7(2)
O6-Li2-O4	89.12(19)	O10-Li2-O4	105.6(2)	O9-Li2-O4	119.4(2)
O6-Li2-Ce1	44.95(11)	O10-Li2-Ce1	127.39(19)	O9-Li2-Ce1	121.74(19)
O4-Li2-Ce1	44.73(10)				